

MEASUREMENT OF THE VERTICAL RADIATION PATTERNS OF
BICONICAL HORN ANTENNAS

A THESIS

Submitted in partial fulfillment
of the requirements for the Degree
of Master of Science in Electrical Engineering

by

John D. Albright

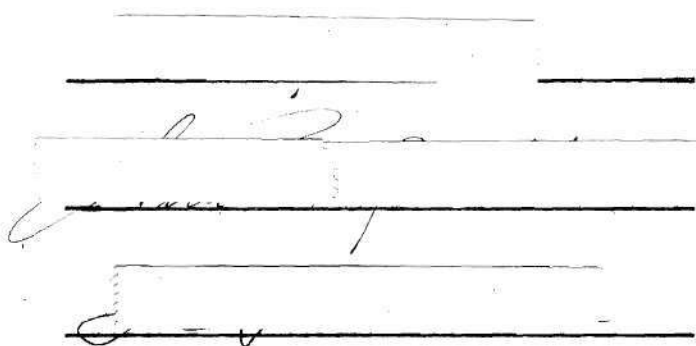
Georgia School of Technology
Atlanta, Georgia
1946

84087

11

MEASUREMENT OF THE VERTICAL RADIATION PATTERNS OF
BICONICAL HORN ANTENNAS

Approved:

A handwritten signature, possibly "J. S. ...", is written across several horizontal lines.

Date Approved by Chairman Nov. 29, 1946

ACKNOWLEDGMENTS

I wish to express my sincerest thanks to Professor M. A. Honnell for his interest in this work and his aid and guidance in its completion. Also, I want to thank Dr. W. A. Edson for his many valuable suggestions and advice.

TABLE OF CONTENTS

	PAGE
Acknowledgments	iii
List of Figures	v
List of Symbols	vii
Introduction	1
Apparatus and Methods of Measurement	4
Discussion of Radiation Patterns	45
Discussion of Input Impedance	50
Conclusions and Recommendations	61
BIBLIOGRAPHY	64
APPENDIX	66

LIST OF FIGURES

Figure	Page
1 General View of Apparatus	5
2 General Layout of Receiving and Biconical Antennas	6
3 Mounting of Biconical Antenna	6
4 Apparatus Setup for Measuring Wavelength	8
5 Detail of Slotted Line	10
6 Detail of Receiving Antenna	11
7 Assembled and Exploded View of Coaxial Detector	13
8 Correction Curves for Slotted Line Detector	15
9a Calibration Curve of Slotted Line Detector	16
9b " " " " " "	17
10 Correction Curves for Receiving Detector	19
11a Calibration Curve of Receiving Detector	20
11b " " " " "	21
12 General Biconical System	22
13 Detail of Mounting of Cones	24
14 Close-up of Antenna and Detuning Sleeve	25
15 Close-up of Cone Pairs	26
16 Vertical Radiation Pattern, $\theta = 0^\circ$	29
17 " " " $\theta = 10^\circ$, $s = 2.5$ cm.	30
18 " " " $\theta = 20^\circ$, $s = 2.7$ cm.	31
19 " " " $\theta = 30^\circ$, $s = 2.9$ cm.	32
20 " " " $\theta = 40^\circ$, $s = 3.4$ cm.	33
21 " " " $\theta = 50^\circ$, $s = 4.2$ cm.	34

LIST OF FIGURES (Continued)

Figure		Page
22	Vertical Radiation Pattern, $\theta = 60^\circ$, $s = 5.2$ cm.	35
23	" " " $\theta = 70^\circ$, $s = 7.4$ cm.	36
24	" " " $\theta = 80^\circ$, $s = 14.6$ cm.	37
25	" " " $\theta = 20^\circ$, $s = \frac{\lambda}{4}$	38
26	" " " $\theta = 30^\circ$, $s = \frac{\lambda}{4}$	39
27	" " " $\theta = 40^\circ$, $s = \frac{\lambda}{4}$	40
28	" " " $\theta = 50^\circ$, $s = \frac{\lambda}{4}$	41
29	" " " $\theta = 60^\circ$, $s = \frac{\lambda}{4}$	42
30	" " " $\theta = 70^\circ$, $s = \frac{\lambda}{4}$	43
31	" " " $\theta = 80^\circ$, $s = \frac{\lambda}{4}$	44
32	" " " $\theta = 50^\circ, 20^\circ$	47
33	" " " $\theta = 70^\circ, 10^\circ$	48
34	Standing Waves in Slotted Line, $\theta = 40^\circ$, $s = \frac{\lambda}{4}$	51
35	" " " " " $\theta = 80^\circ$, $s = 14.6$ cm.	52
36	Characteristic Impedance of Biconical Horn Antenna	58
37a	Biconical Antenna System	59
37b	Equivalent Circuit of Biconical Horn Antenna	59

LIST OF SYMBOLS

Symbol	Meaning
a	Diameter of Inner Conductor of Coaxial Line
α	Attenuation Constant
β	Phase Constant
b	Inner Diameter of Outer Conductor of Coaxial Line
b_m	A Coefficient
d	Distance of Detuning Sleeve Below Cone on Slotted Line
ϵ	Dielectric Constant
$F(k_1)$	A Function
$G(k_1)$	A Function
j	$\sqrt{-1}$
$J_p(x)$	Bessel Function of the First Kind
k	$\frac{2\pi}{\lambda}$
l	Distance on Slotted Line
l	Length of Line in Equivalent Circuit of Biconical Antenna
λ	Wavelength
\ln	Natural Logarithm
μ	Permeability of Dielectric
n	An Integer
$N_p(x)$	Bessel Function of the Second Kind
π	3.14159...
r	Voltage Standing Wave Ratio
s	Slant Height of Cones
θ	Angle of Flare of Cones

LIST OF SYMBOLS (Continued)

Symbol	Meaning
Z	An Arbitrary Load
Z_L	Load in Equivalent Circuit of Biconical Antenna
Z_0	Characteristic Impedance

MEASUREMENT OF THE VERTICAL RADIATION PATTERNS OF BICONICAL HORN ANTENNAS

INTRODUCTION

From an analytical point of view, antenna systems in which two cones mounted coaxially tip to tip with a very small gap between apices as shown in Fig. 12 on page 22 have been investigated by several authors¹ in recent years. In these works the biconical system is considered both as a transmission line, made up of two cone shaped wires leading off in opposite directions and fed at the center, and also as an antenna of the dipole type. Both approaches are useful, depending on the information desired. The biconical systems used in this work are looked at mostly from the point of view of their being antennas, but the transmission line approach is necessary in determining their characteristic and input impedances.

A biconical horn antenna fed by a coaxial line may be visualized as developed in two ways. A rectangular electromagnetic horn which is flared horizontally and vertically may be thought of as attached to a very short section of rectangular wave guide coupled to a coaxial line so as to feed the horn in the $TE_{0,0}$ mode. Now, if the horizontal flare is made to increase to 360° about the center conductor

1. W. L. Barrow, L. J. Chu, and J. J. Jansen, "Biconical Electromagnetic Horns," Proc. I. R. E., 27, 769, Dec., 1939. S. A. Schelkunoff, "Theory of Antennas of Arbitrary Size and Shape," Proc. I. R. E., 29, 493, Sept., 1941. J. A. Slater, "Microwave Transmission," pp. 202-205, McGraw-Hill Book Co., N. Y., 1942. S. Ramo and J. R. Whinnery, "Fields and Waves in Modern Radio," pp. 421-425, John Wiley & Sons, N. Y., 1944.

of the coaxial line, while the vertical flare remains the same we will have generated a pair of cones to form the biconical antenna. Again, if we think of a coaxial, half-wavelength, dipole antenna and allow the inner conductor and the outer sleeve to swell up to cones, we have again the desired antenna system. It is this last method of visualization that will be used in this paper.

Judging from the literature, it would seem that there has been very little work done on actual cones to measure experimentally their radiation patterns and input impedances. Moreover, in the experimental work that has been done, the slant height of the cones was long compared to the wavelength employed.² By this means very sharp and well directed horizontal lobes were obtained. This leads one to suppose that biconical horn antennas may be used for broadcast purposes. In the microwave region this has been done.³

Due to the mechanical simplicity of antennas of this type, it would be very desirable to have them operate at much lower frequencies and still retain their horizontal beam characteristics. To work at lower frequencies, or longer wave lengths, the cones must be scaled up in physical size.⁴ If it were desired to drive a biconical horn antenna at about 100 megacycles for frequency modulation broadcast work and still maintain the ratio of slant height to wavelength

2. Barrow, W. L., op. cit.

3. M. I. T. Radiation Laboratory Report 263 (54-15)
 "Horizontally Polarized, 9.1 cm. Biconical Horn Beacon Antenna"

4. J. A. Stratton, "Electromagnetic Theory," pp. 488-490,
 McGraw-Hill Book Co., N. Y.

at 5.7 as used by Barrow, it would demand a set of cones having a base diameter of about 86.5 feet.

It is the purpose of this paper, therefore, to make an experimental investigation of the radiation patterns of biconical horn antennas having a slant height small compared to the wavelength used. A large part of the work was done using $s = \frac{\lambda}{4}$. Here λ is the wavelength in centimeters and s is the slant height of the cones.

APPARATUS AND METHODS OF MEASUREMENT

In Figs. 1, 2 and 3 on pages 5 and 6, the general appearance and physical layout of the apparatus is shown. The Klystron in the rolling cabinet in the left of Fig. 1 has been in use in the Electrical Engineering Department for some time, and required very little effort to put it in good working order. It was found that using an accelerator anode voltage of about 875 volts sufficient power output could be obtained to make all the necessary measurements. The Klystron tube used had a rating of about 3 watts output with approximately 2,000 volts on the accelerator anode and a beam current not exceeding 30 milliamperes. The 60 cycle power input to the Klystron came through a voltage regulating transformer, but most of the fluctuations noticed in the output were not removed until the metal frame of the cabinet was grounded.

The tube had previously been tuned to a wavelength of 9.920 centimeters, and in view of the difficulties involved in retuning, it was decided to use this wavelength throughout all the work. A measurement of the wavelength was made before any of the other recorded data was taken, and this measurement was repeated every day or so during the experimental period. A coaxial wavemeter capable of measuring to 0.001 centimeter was used. A sliding plug driven by a micrometer screw formed a tunable cavity resonator in a section of coaxial line, allowing transmission from the input probe to the output loop when the plug was a whole number of half-wavelengths from the input end. A microammeter connected to the crystal detector on the output

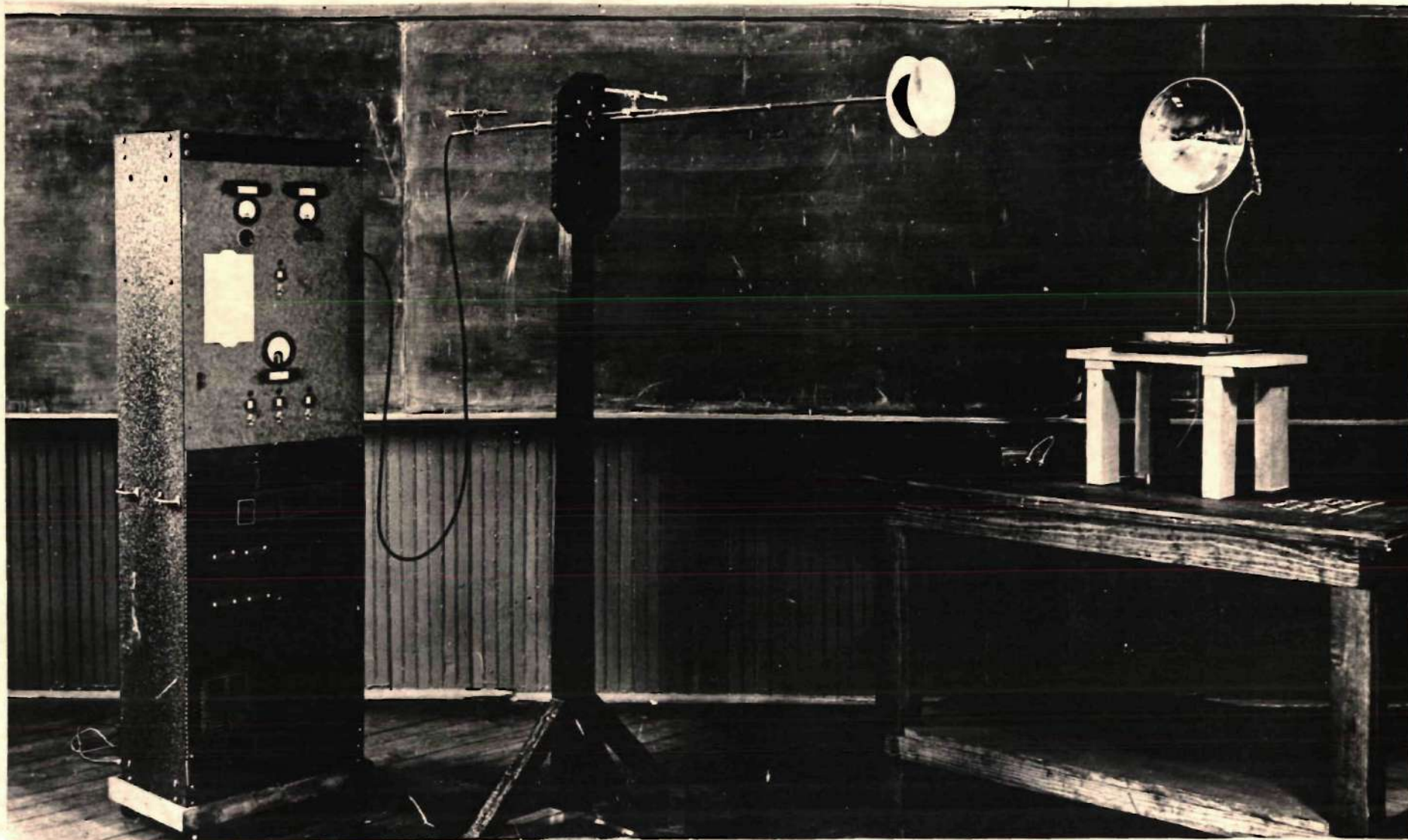


FIGURE 1
General View of Apparatus
Showing Klystron cabinet, slotted on revolving mounting with 70° cones, and receiving
antenna

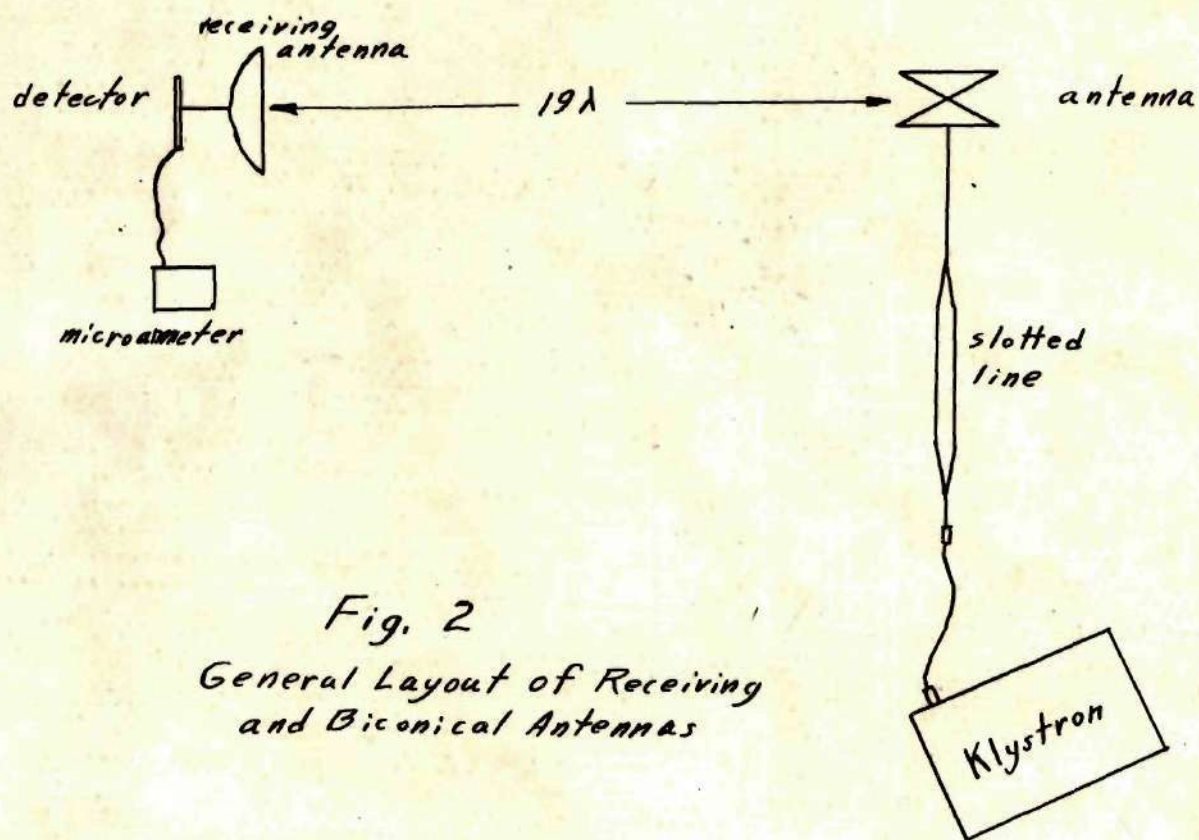
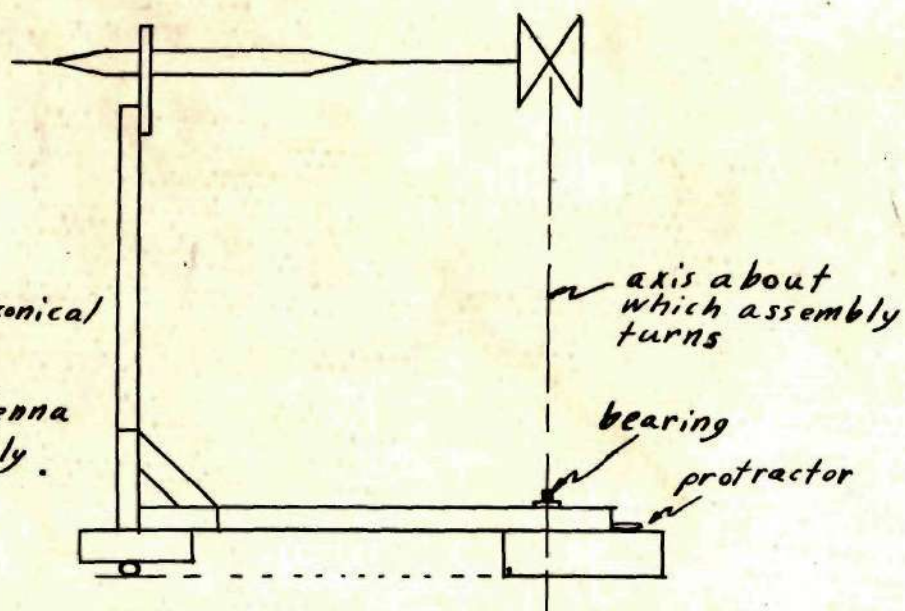


Fig. 2
General Layout of Receiving
and Biconical Antennas

Fig. 3
Mounting for Biconical
Antenna

Showing how antenna
is mounted directly
above axis of
rotation



loop indicates transmission through the cavity, and the difference in the wavemeter dial settings for two successive transmission points is one-half wavelength. This apparatus is shown in Fig. 4, page 8.

Because beaded coaxial cable with plugs and connectors was already available for use with the $3/8$ inch, 55 ohm, rigid coaxial line used in the Electrical Engineering Department, it was decided to design the antenna cones to be attached to this size line. However, the spacing between the inner and outer conductors of the $3/8$ inch line was so small that probing into it for voltage standing wave ratio measurements would have been difficult. For this reason, an enlarged section of 55 ohm line was built, having a radial distance between inner and outer conductor of 0.229 inches. The outer conductor of this section was standard $7/8$ inch copper tubing. To allow space for mounting and for a probe slot of 1.5λ the large section was made three wavelengths long. To match this section to the smaller $3/8$ inch line, a tapered section three wavelengths long was used at each end. The taper of the outer conductor was made of sheet copper, rolled on a mandril. The inner conductor was also tapered in the same way, having a maximum diameter of 0.306 inches and tapered down at each end to 0.125 inches. The middle section with the two tapered ends was turned in one piece from copper. The $1/8$ inch diameter extensions on each end were of brass rod, silver soldered in place. All other seams and joints were made with silver solder. The inner conductor was supported in place by polystyrene insulator rings, spaced about six inches apart along the small section of the line and one at each end of the large section next

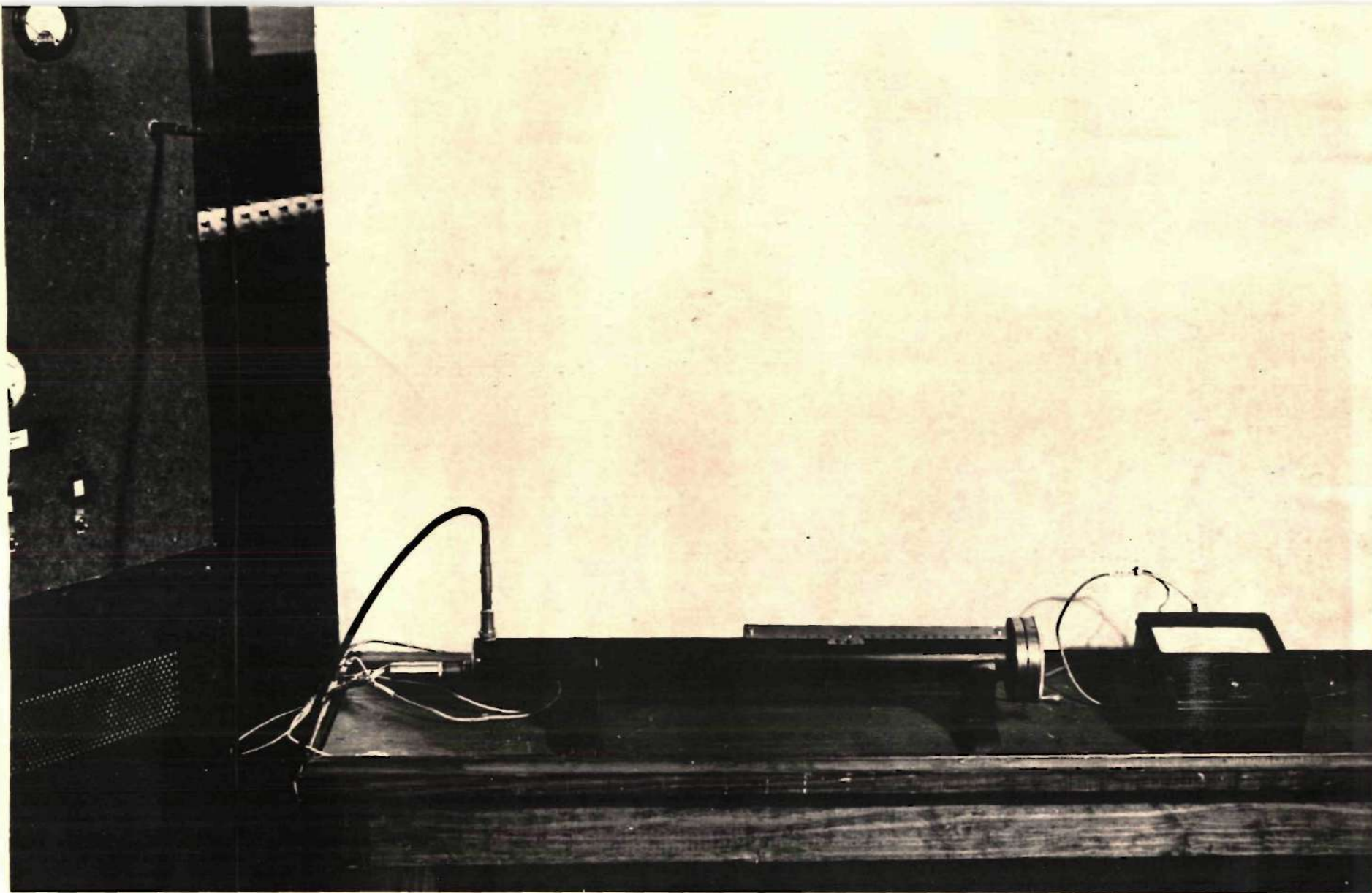


FIGURE 4
Apparatus Setup for Measuring Wavelength
Showing coaxial wavemeter coupled to Klystron and detector wired to meter

to the base of the taper. The exterior details are shown in Fig. 1 on page 5, and Fig. 5 on page 10.

The whole slotted line was mounted horizontally on a wooden frame which allowed the antenna on the end of the line to be rotated about an axis passing through the center of the antenna. See Figs. 1 and 3. If the receiving antenna is held in a fixed position it gives the effect of the radiating antenna being fixed and the receiving antenna rotating about it at a constant radius in the vertical plane. Unfortunately, the bearing on which the wooden mounting frame revolves is not shown in Fig. 1.

The receiving antenna is shown in detail in Fig. 6 on page 11. This consists of a parabolic reflector holding a center fed half-wavelength antenna on a section of 55 ohm coaxial line. The antenna is oriented horizontally and has a $\frac{\lambda}{4}$ detuning sleeve directly below on the coaxial line. Projecting in front on a polystyrene rod is a parasitic reflector. While the parabolic reflector is fairly large, it causes little interference with the radiation pattern of the antenna being tested as its position is fixed during all measurements.

Three crystal detectors were used in this work. One was used to monitor the field coming into the slotted line, another for the voltage standing wave ratio (v.s.w.r.), and the third was for the receiving antenna detector. These detectors are all of the same design and were made principally of standard size brass and copper tubing. The crystal rectifier itself is of the newer microwave type

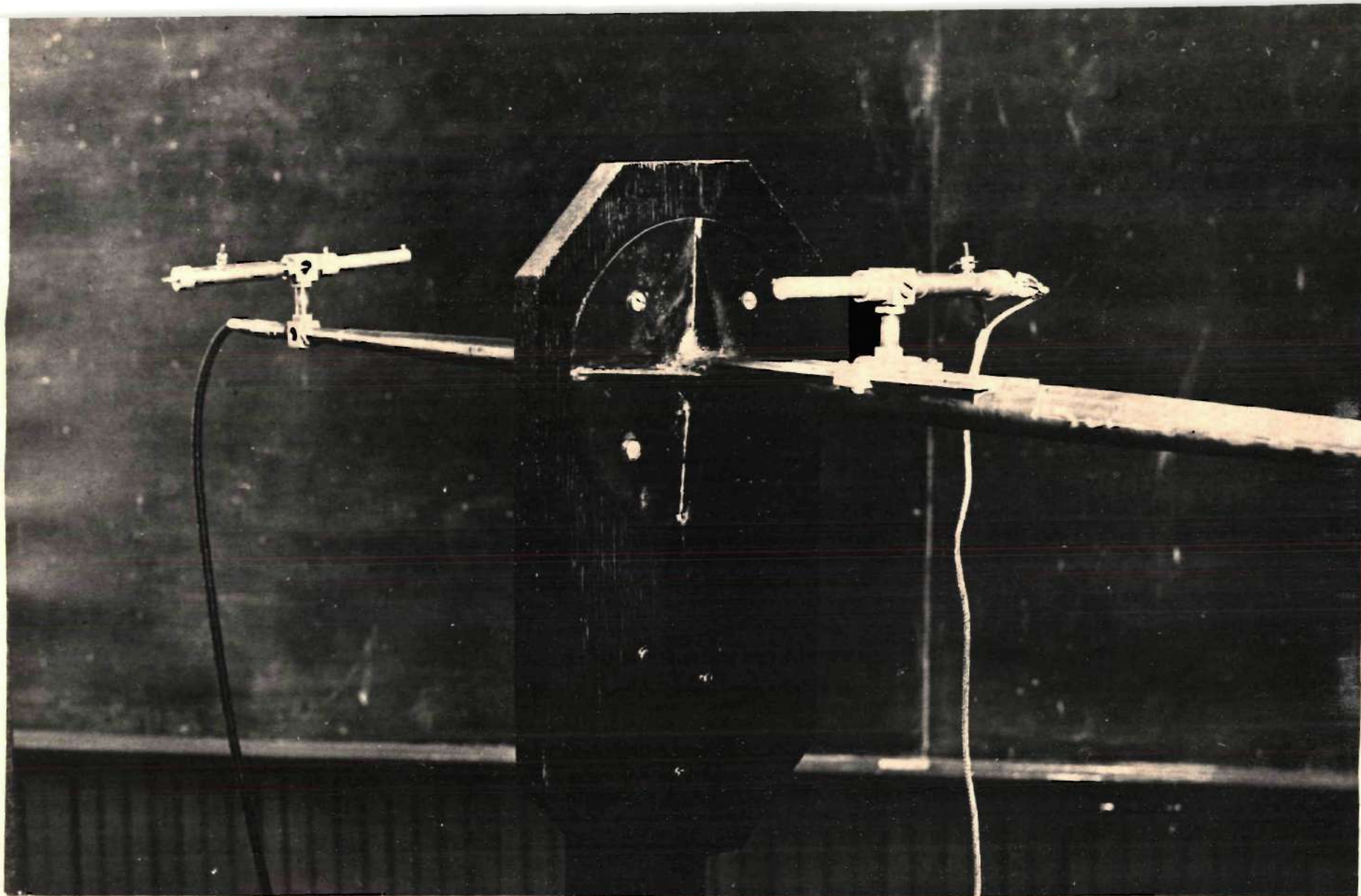


FIGURE 5
Detail of Slotted Line
Showing the sliding probe and the monitoring detector

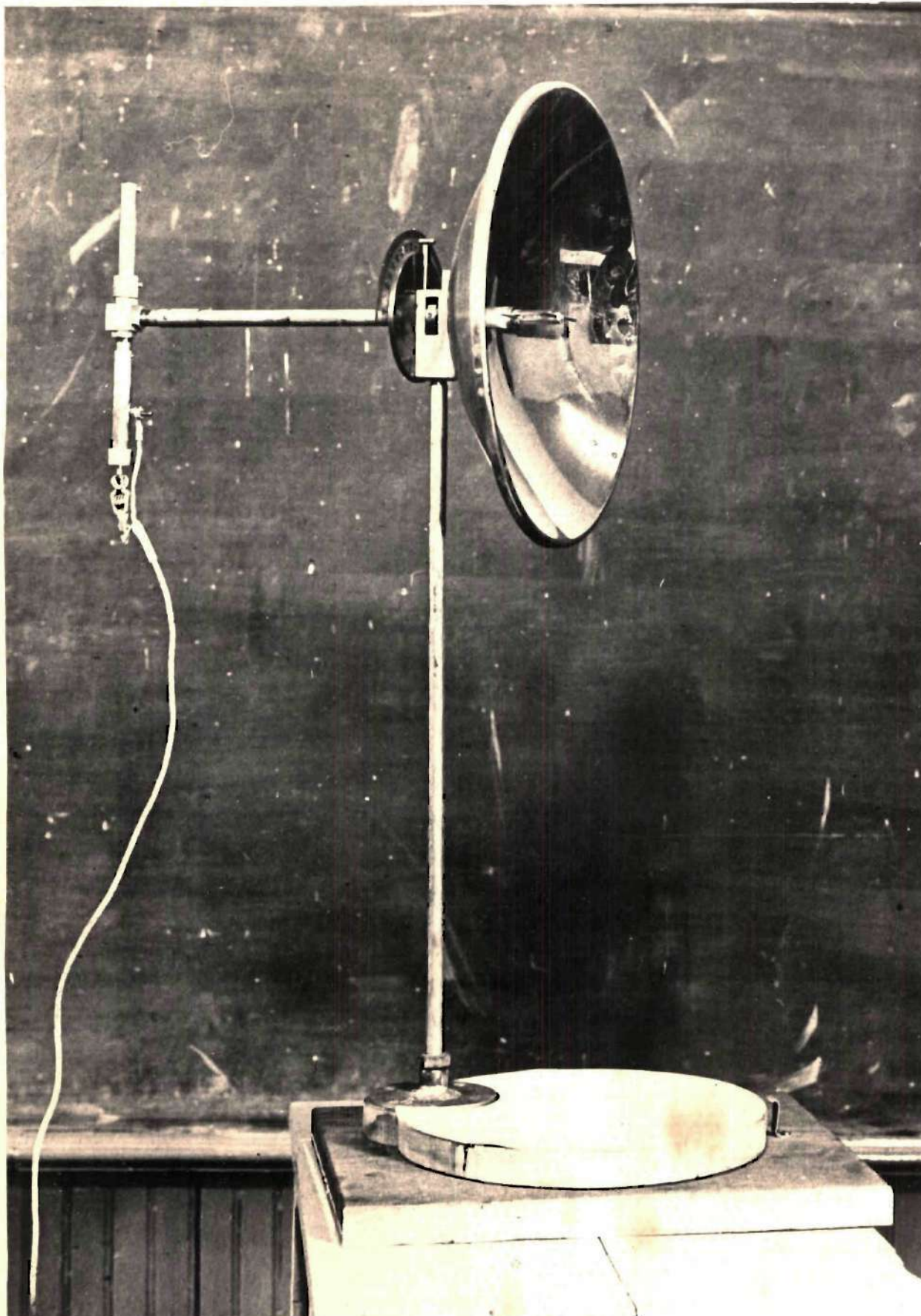


FIGURE 6
Detail of Receiving Antenna

permanently mounted in a ceramic cartridge.⁵ The crystal itself is the fourth part from the left in Fig. 7 on page 13. This assembly consists of a junction block with a coaxial tuning stub mounted on one side and the crystal mounted as part of the inner conductor of a section of a coaxial line on the other side. The pickup probe is shown below the junction block. The inner conductors form a T-joint inside the block. The cylindrical plug at the left of the crystal in Fig. 7 forms with the outer conductor a coaxial condenser to short out the r.f. which passes the crystal. The projection on the outer conductor and the rod on the end of the condenser plug form the direct current connections.

Because the amplitude response of the crystal detector is non-linear, it is necessary to get a calibration for the v.s.w.r. detector on the slotted line and the receiving antenna detector. Crystals of the type used ordinarily have a square law response; but as will be seen later, if such an assumption is made in all cases, it will lead to a serious error. To calibrate the v.s.w.r. detector, the end of the coaxial line on which the antennas are mounted is shorted. In this case, the short consisted of a doughnut-shaped roll of aluminum foil pressed tightly against the opening of the line in the space between the inner and outer conductors. Next, a scale was marked on the sliding probe's ways. The units were 0.1 inch apart. It was found that this unit distance would be easier to mark and read than unit

5. A. Peterson, "Vacuum-tube and Crystal Rectifiers as Galvanometers and Voltmeters at Ultra-high Frequencies," General Radio Experimenter, Vol. 29, No. 12, May, 1945.

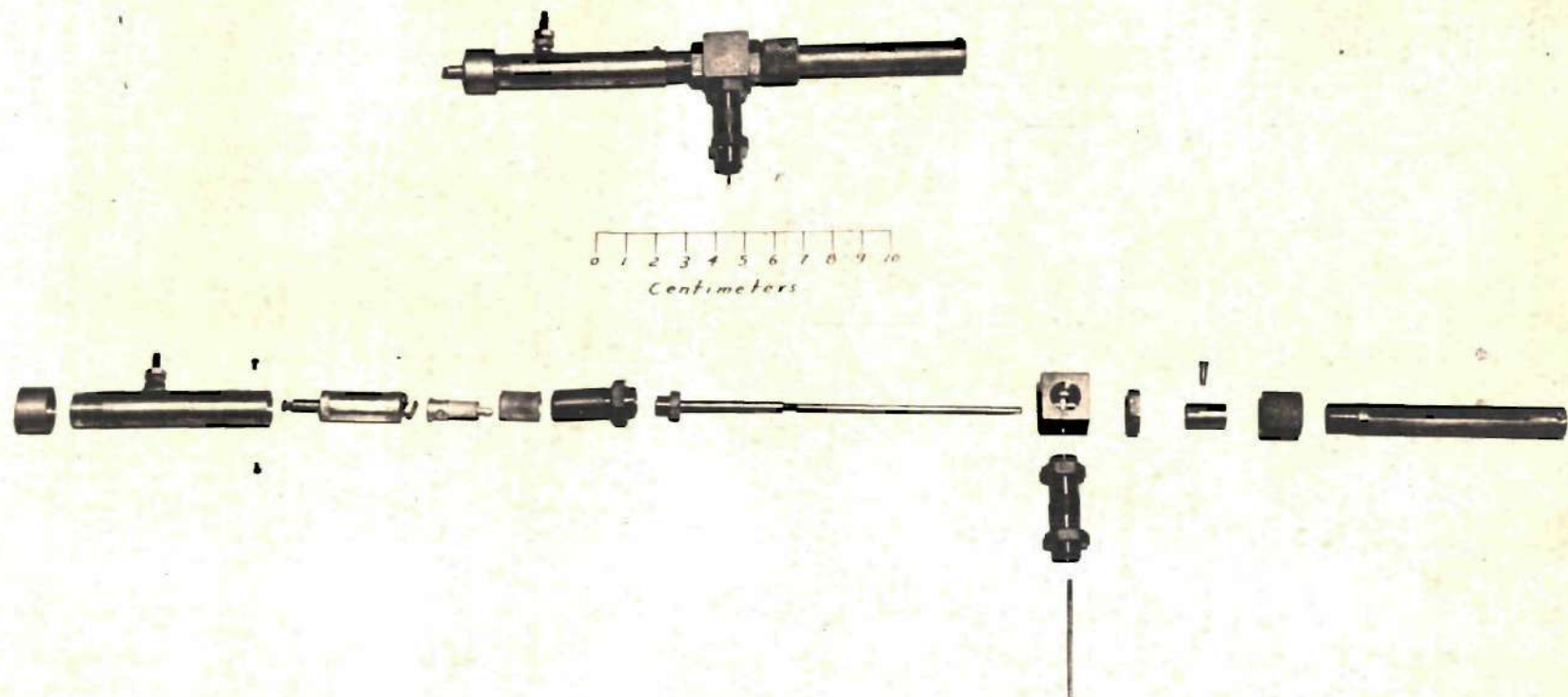


FIGURE 7
Assembled and Exploded View of Coaxial Detector
Crystal is forth from left in exploded view

distances of one millimeter. The v.s.w.r. detector probe was set at a fixed depth of about 4 millimeters into the inter-conductor space of the line. As the probe assembly (see Fig. 5, page 10) was moved back and forth on the slot ways positions of maximum and zero field were found. It was noted that the zero points occurred at marks 9 and 29 on the probe scale. According to this measurement, a half-wavelength would be two inches long. On the basis of a 10 centimeter wave, this means an error of 0.3 of a scale division in the placement of the voltage nodes by the probe. The fact that the voltage did go to zero at some positions indicates that the Klystron's output was a fairly pure sine wave. Measurements of the field strength appearing as a rectified direct current were taken for each marked position along the slot.

This data was normalized and plotted on Fig. 8 on page 15. If the crystal response had been linear, the curve of measured current would have been pure sine curve; assuming, of course, that the voltage standing waves in the line were sine curves. The actual resulting curve, however, is plotted on the same base as a sine curve, and the difference in the two curves gives the degree of nonlinearity of the crystal response. To find the true or corrected value of crystal current, points are taken on the measured current curve in Fig. 8 and projected up to the sine curve. The corresponding values of these points give the true or corrected current. Fig. 9a on page 16 shows the amplitude response curve of the crystal plotted as measured current versus true current. Fig. 9b on the next page gives the same curve plotted on log-log paper. This shows that the original curve

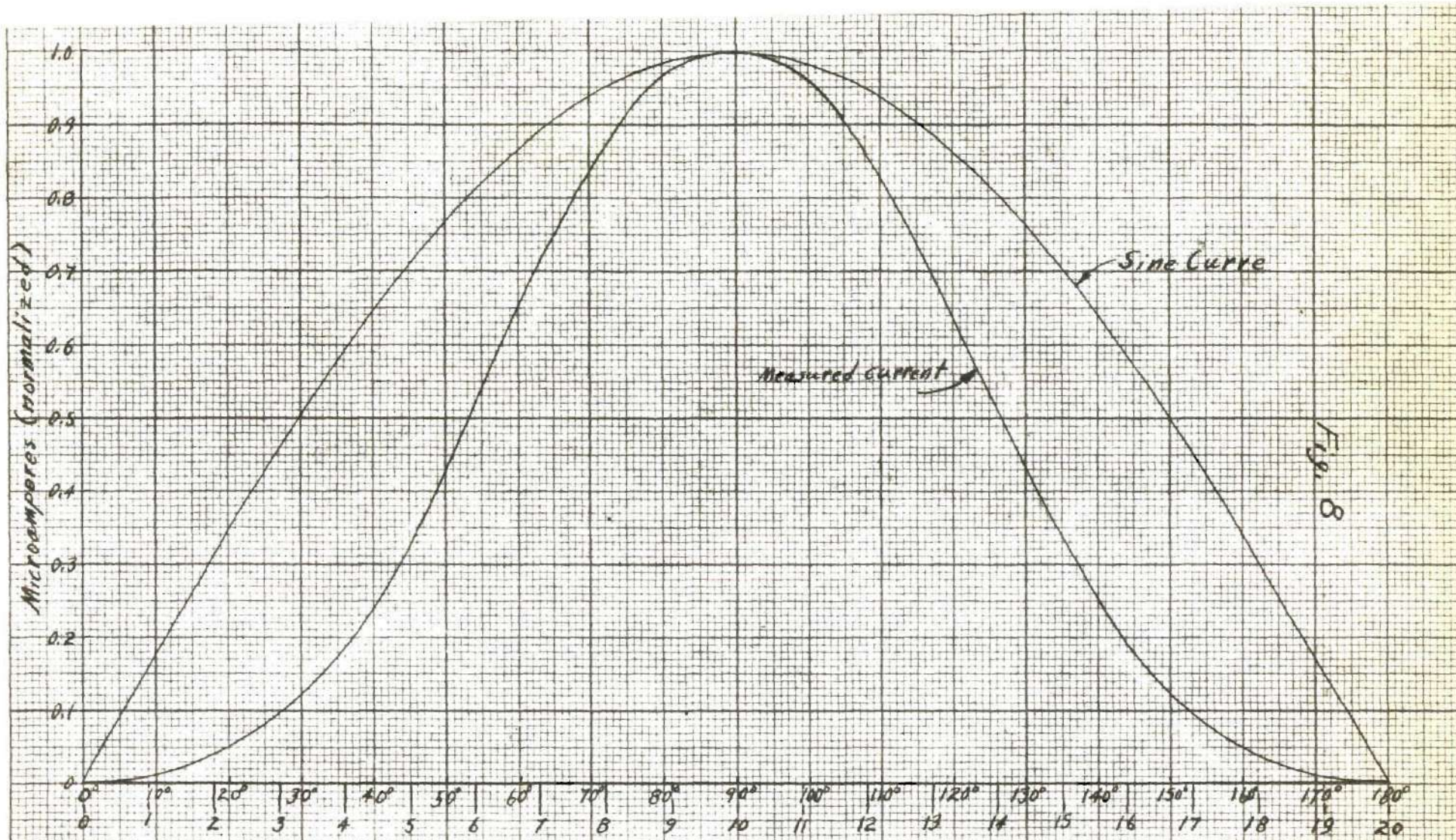


Fig. 8

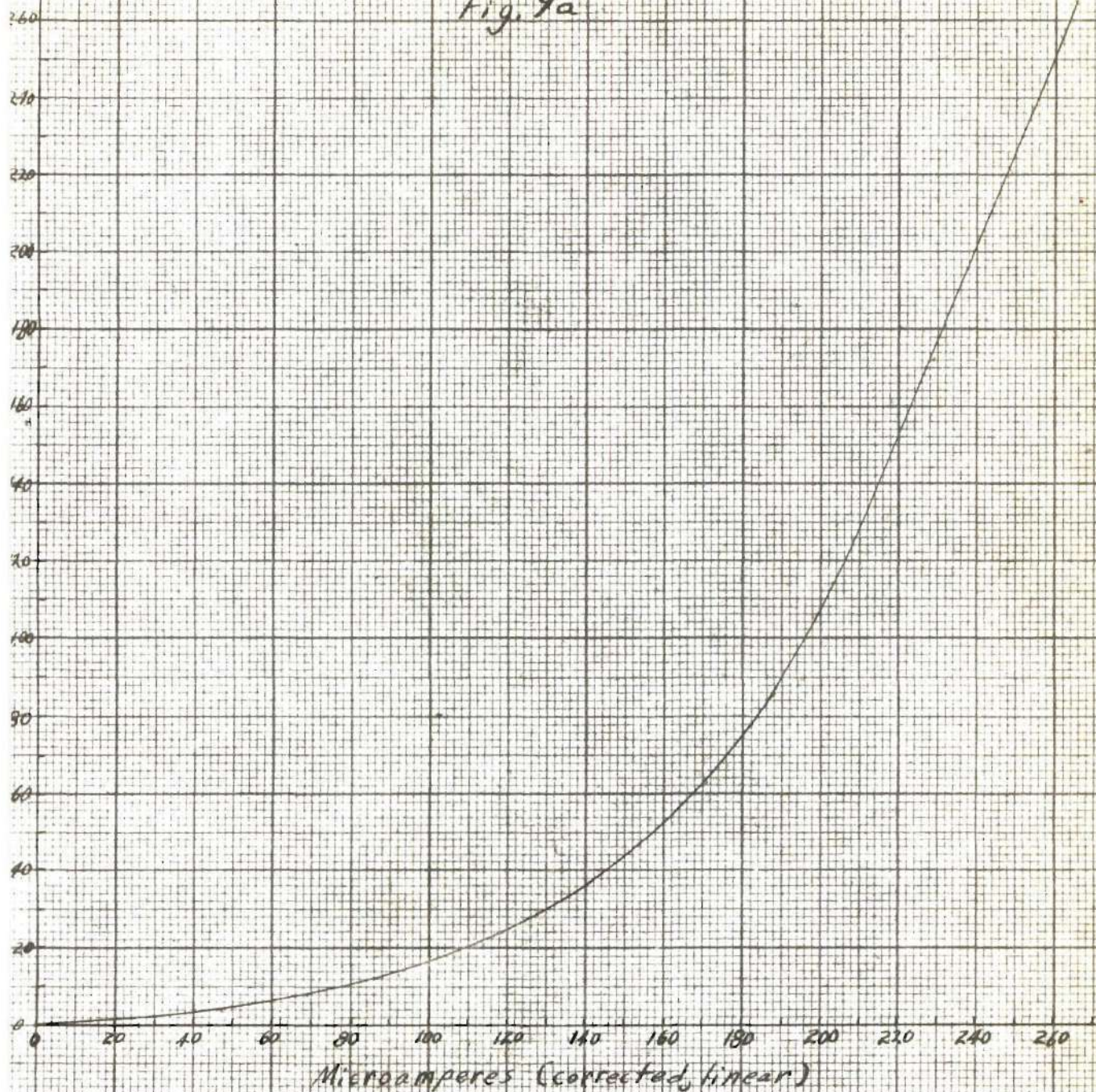
Electrical Degrees and Units of Distance along Slotted Line

Maximum current = $265 \mu a$

Correction Curves for Slotted Line Detector

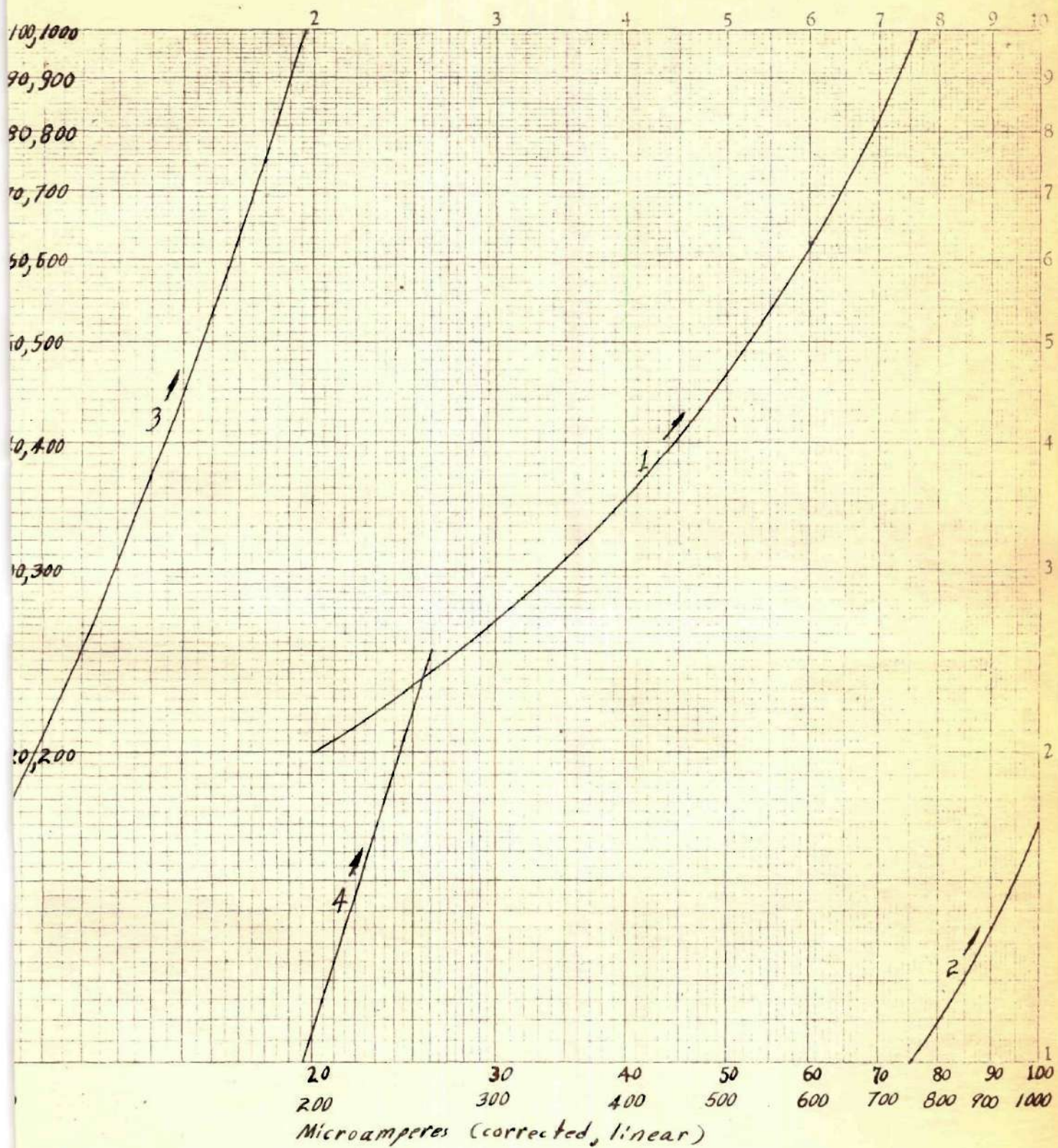
J.P.A.

Fig. 9a



Calibration Curve of
Slotted Line Detector

J.R.A.



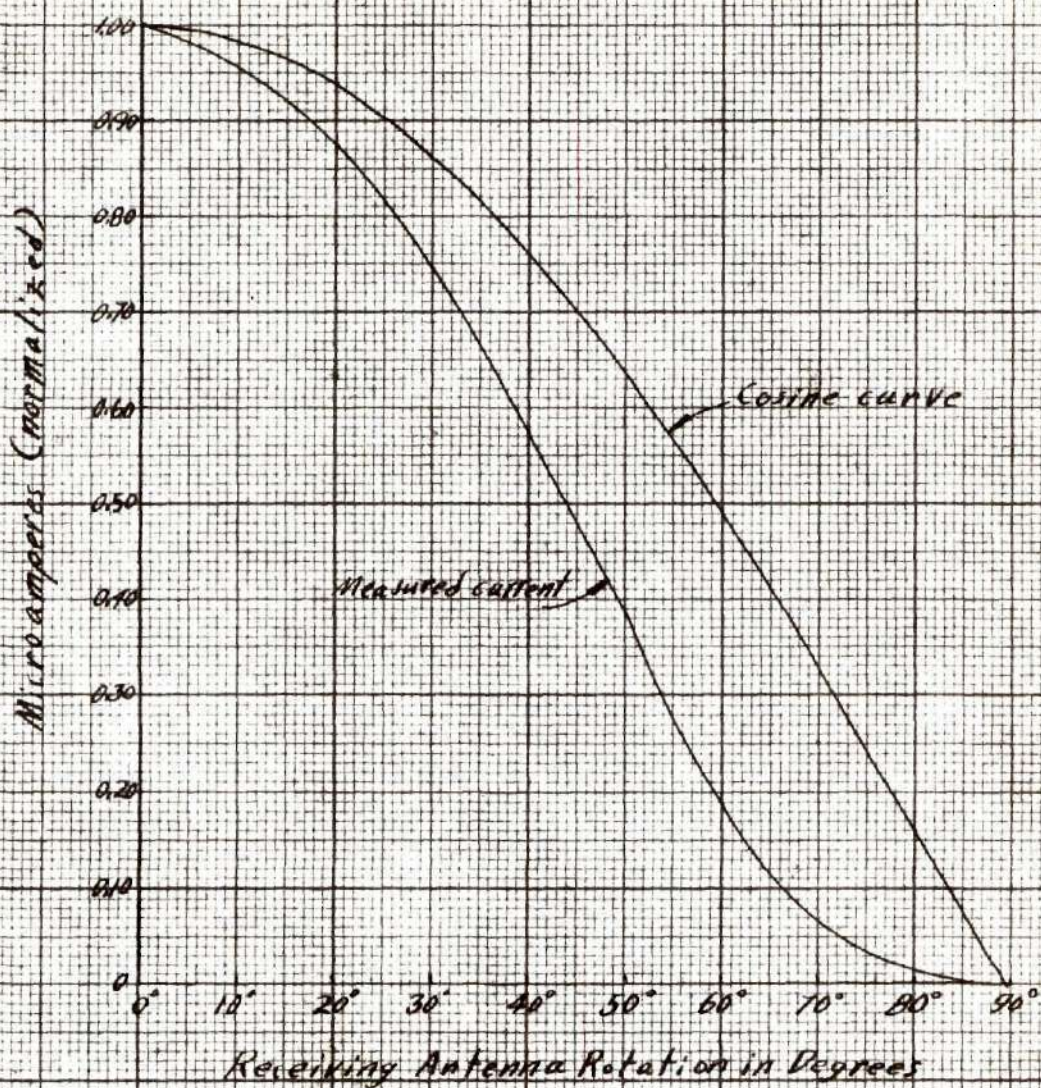
Calibration Curve of
Slotted Line Detector

is far from exponential.

The receiving antenna detector is calibrated in a manner similar to the above. A polarized field was first obtained, using one of the biconical antennas. As these antennas produce polarization parallel to their axis, a horizontally polarized field resulted when they were mounted on the slotted line. The receiving antenna was then turned to intercept a maximum of the incoming field. A pointer on the receiving antenna's coaxial feed line was then set to the zero mark on the protractor shown in Fig. 6. The current induced into the half-wavelength receiving antenna by the incoming field is proportional to its effective length. This effective length is in turn proportional to the cosine of the angle of rotation out of the plane of polarization of the incoming field. The output of a linear detector plotted against the angle of rotation from 0° to 90° would, therefore, produce a section of a cosine curve. In Fig. 10 on page 19 is shown the normalized measured detector current plotted on the same base as a quarter-period cosine curve. To obtain the calibration curve of Fig. 11a on page 20 the same procedure was followed as with the v.s.w.r. detector. Fig. 11b is the same calibration curve plotted on log-log paper. Here, one section of the curve has an exponent of 1.58.

The eight pairs of cones used as biconical horn antennas in this work were made of 0.01 inch thick sheet brass. The angle of flare was the same for both cones of each pair and was measured in the same way as in Fig. 12 on page 22. Cones were constructed with angles for every ten degrees from 10° to 80° . The cones were

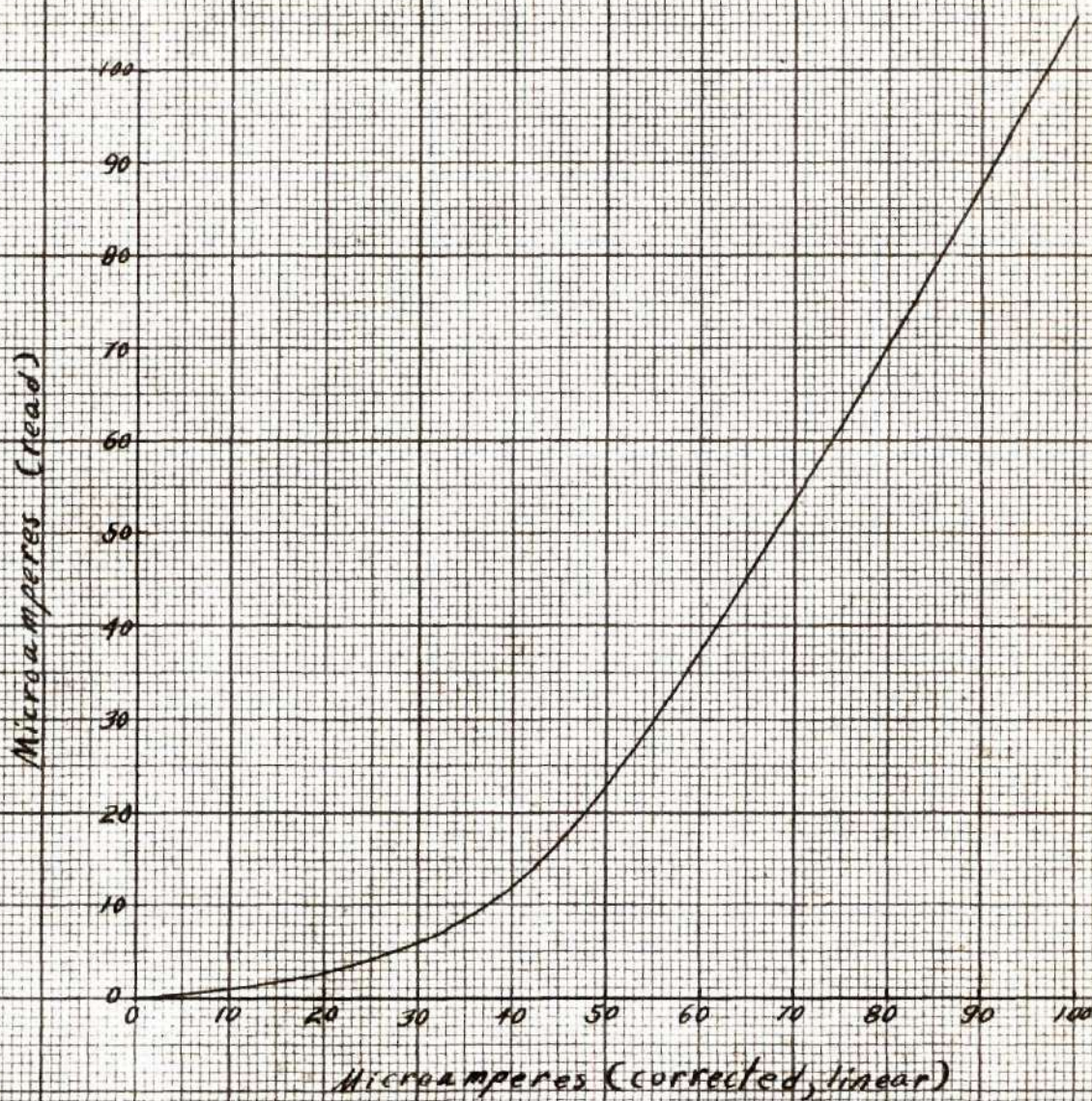
Fig. 10



Maximum current = 92.75 μ A

Correction Curves for
Receiving Detector

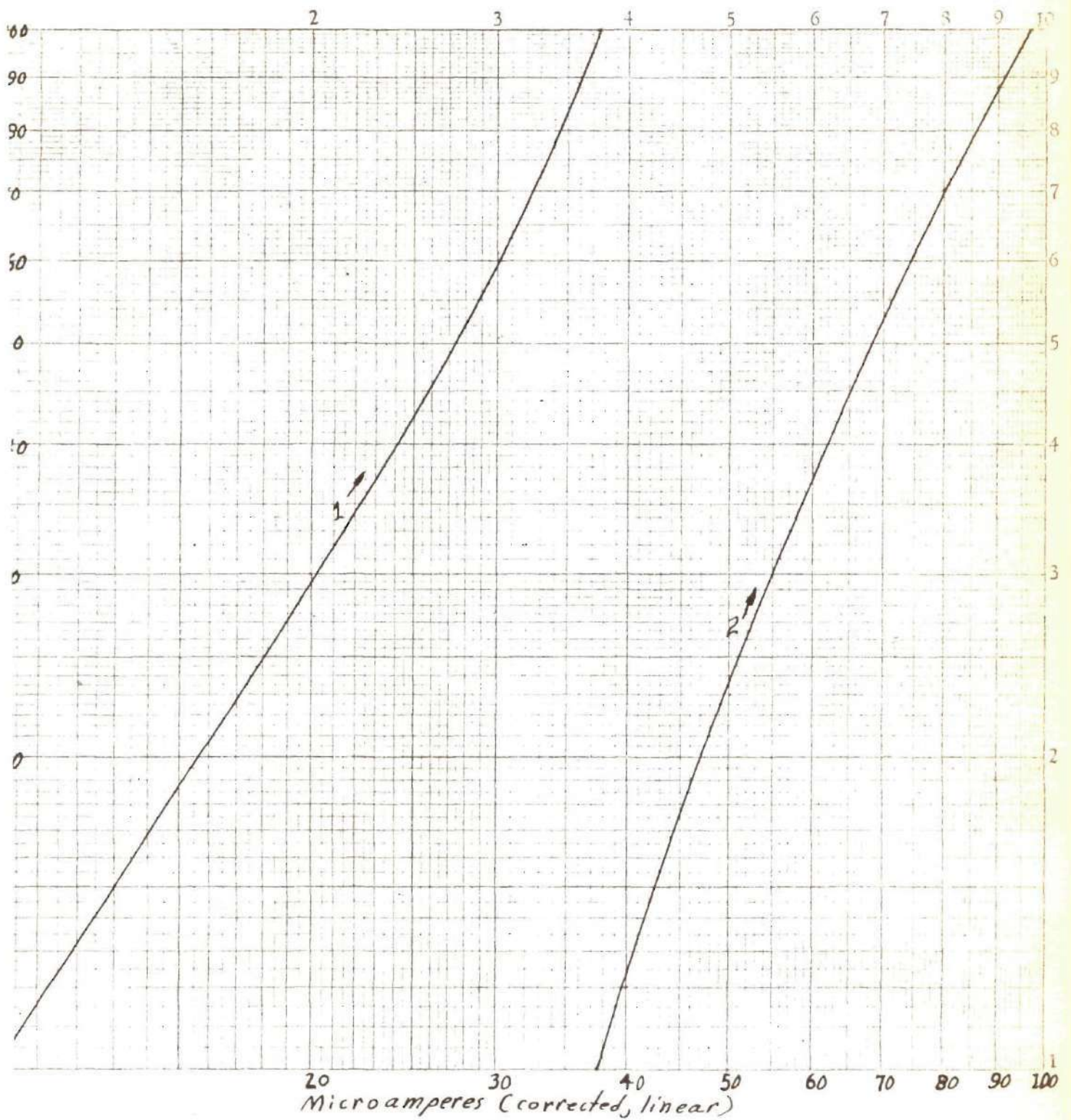
Fig. 11a



Calibration Curve of
Receiving Detector

Fig. 11b

21



Calibration Curve of
Receiving Detector

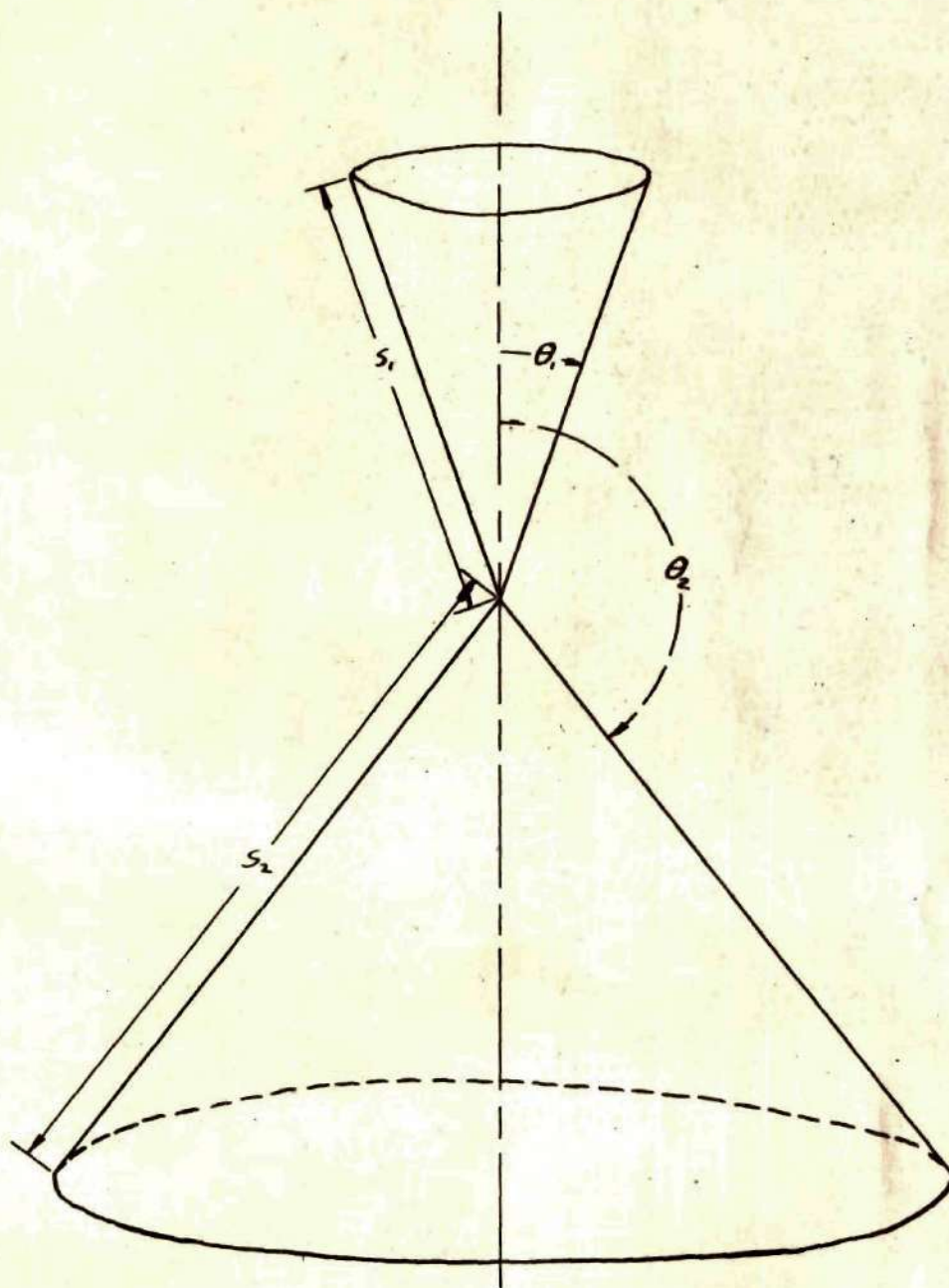


FIGURE 12
General Biconical System

originally made with the vertical height equal to $\frac{\lambda}{4}$. The resulting slant heights are given in Figs. 17 and 24, on pages 30 to 37. After all the measurements were made with the cones in this condition, they were cut down so that s , the slant height, equaled $\frac{\lambda}{4}$. In Fig. 13 on page 24, is shown their mechanical construction and method of mounting on the end of the slotted line. The black marks near the tip of each cone in Fig. 13 indicate a split brass ring used to allow the cone to be fitted tightly to the coaxial line. In Fig. 14 on page 25 is shown the 30° antenna, with $s = \frac{\lambda}{4}$, mounted on the line. A 70° antenna with $s = 7.4$ centimeters is shown in Fig. 1. A number of the cone pairs are shown in Fig. 15 on page 26.

The two important measurements made on the antennas were to determine the radiation pattern and the input impedance. As was said, the cones were originally made with the slant height greater than $\frac{\lambda}{4}$. With the cones in this condition, the radiation pattern was plotted with and without a $\frac{\lambda}{4}$ detuning sleeve on the line below the antennas. Measurements of the v.s.w.r. were made under these two conditions also. The slant height of the cones was then cut down to $\frac{\lambda}{4}$ and all of the above measurements repeated.

To take the data for the radiation pattern, the cones were fitted on the end of the line as shown in Figs. 1, 13 and 14. The wooden frame mounting the slotted line assembly was rotated to the zero mark on the bearing protractor (see Fig. 3). The receiving antenna was placed on a line passing through the bearing, 90° off the axis of the biconical horn system, and at a distance of about 19λ . This position was held fixed during all the measurements. The receiving

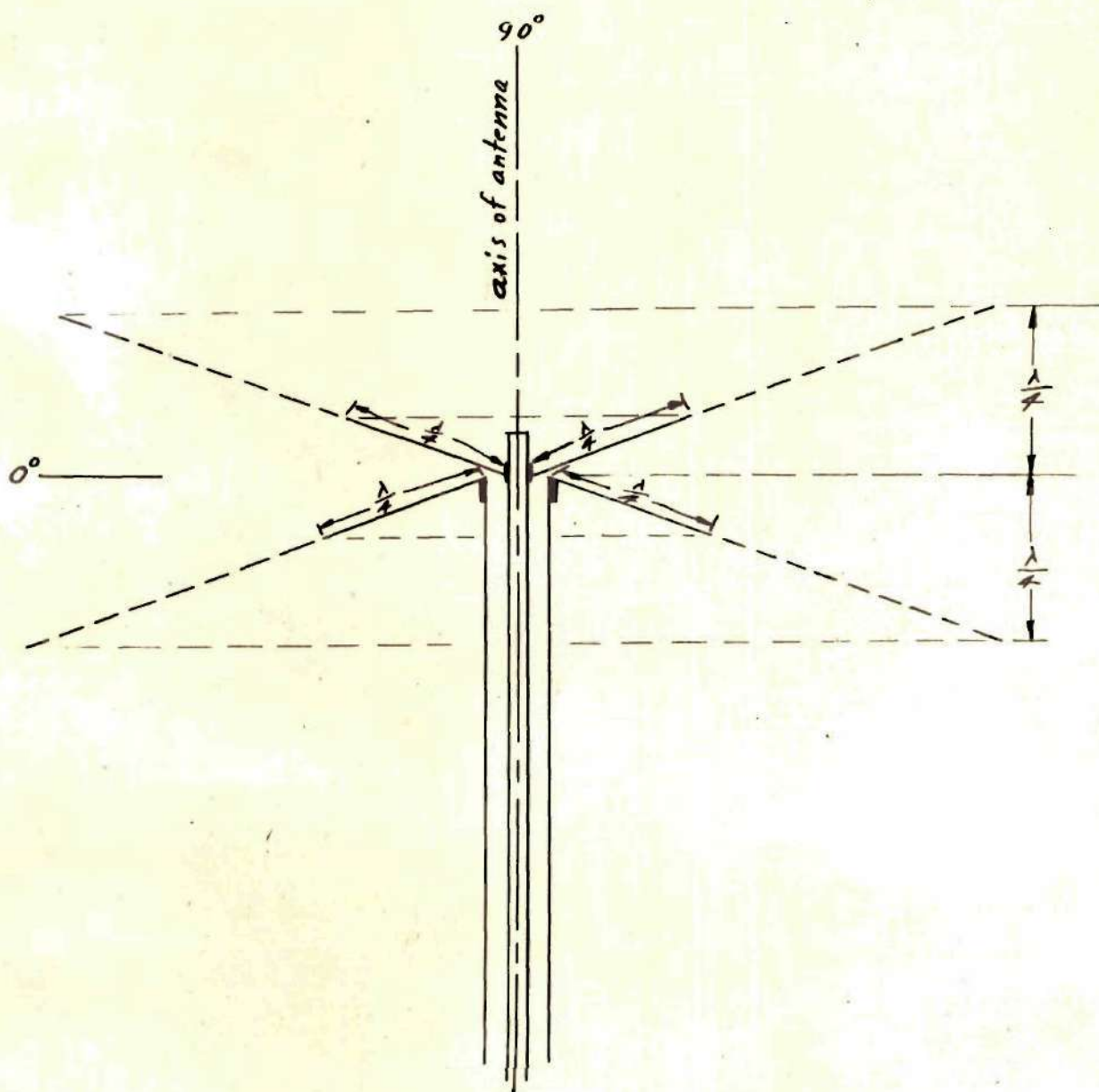


FIGURE 13
Detail of Mounting of Cones

Showing the 70° cones with $s = 7.4$ cm. and
with $s = \frac{\lambda}{4}$ mounted on $3/8$ inch coaxial
line. Full size.



FIGURE 14
Close Up of Antenna and Detuning Sleeve
30° cones with $s = \frac{\lambda}{4}$

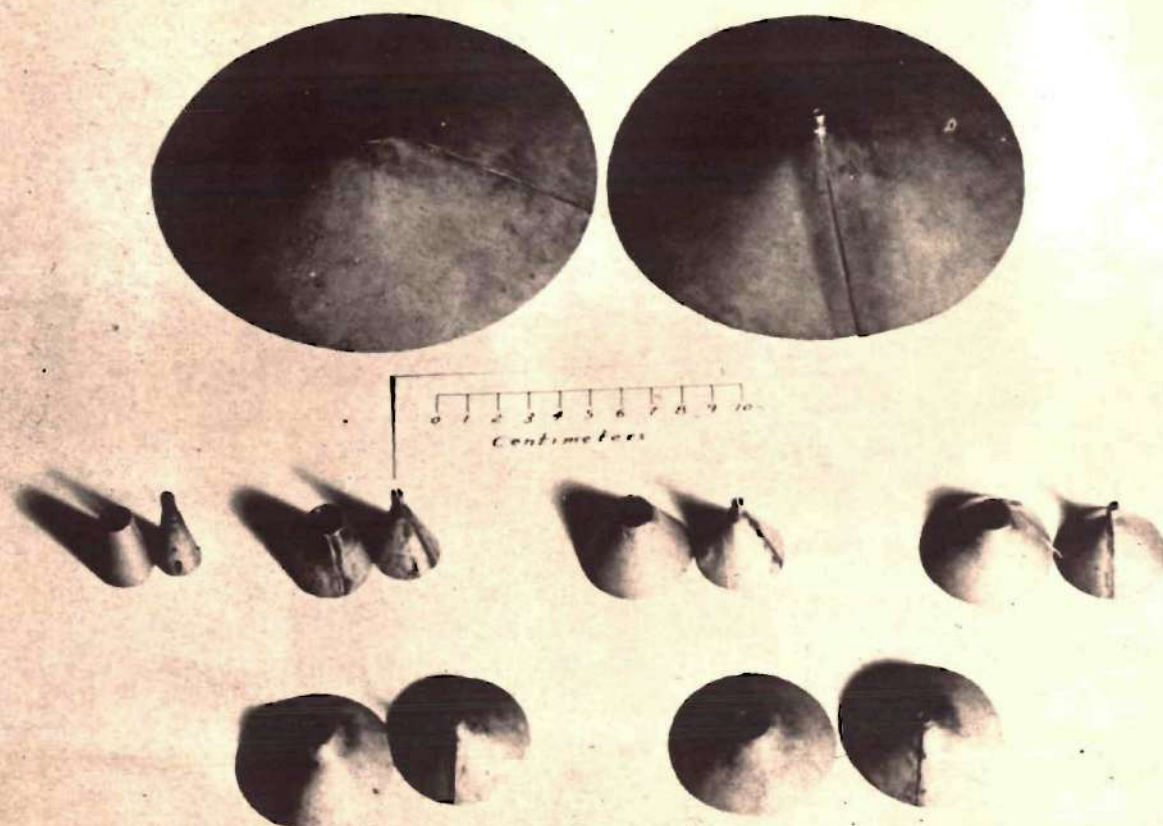
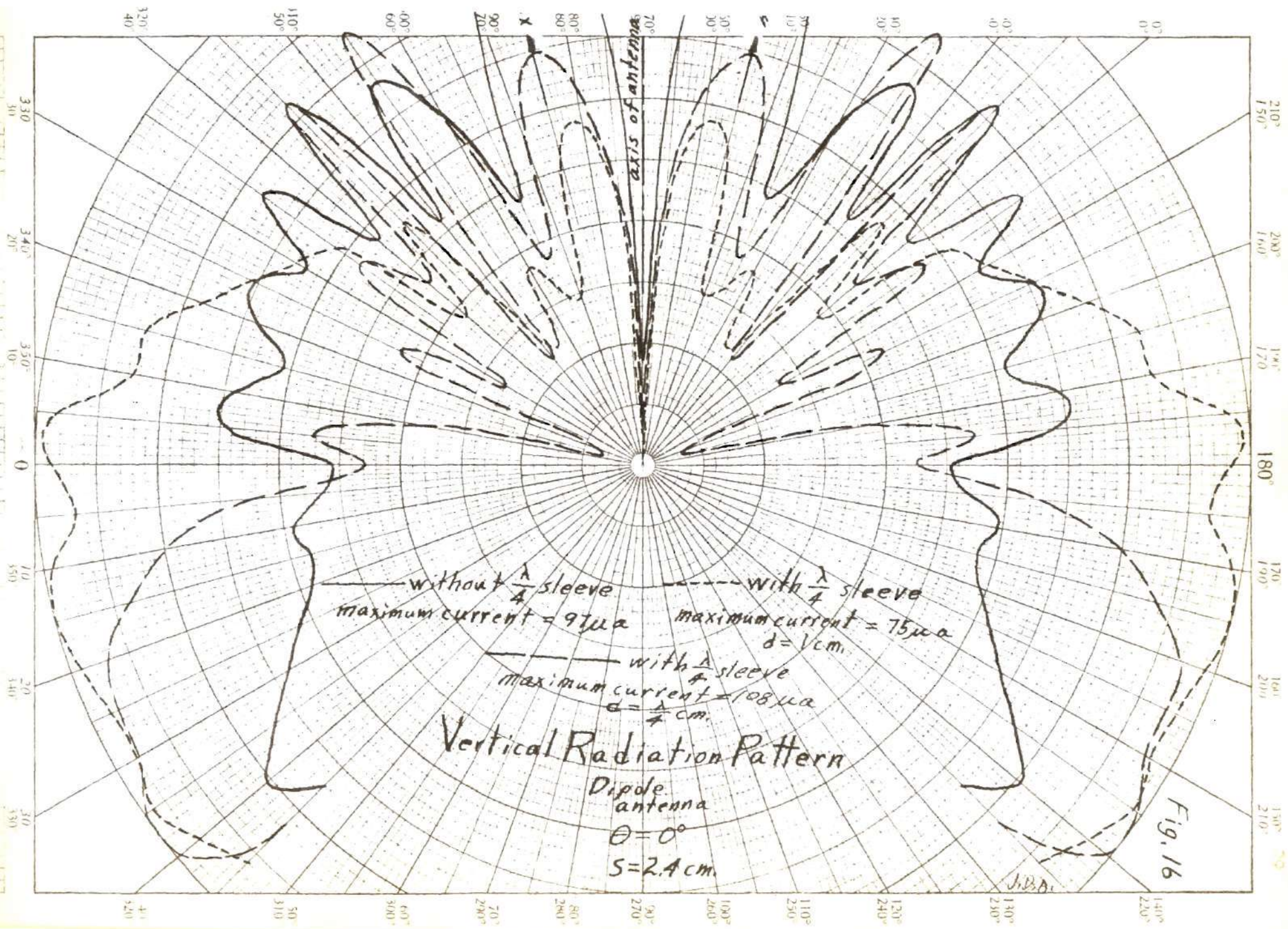


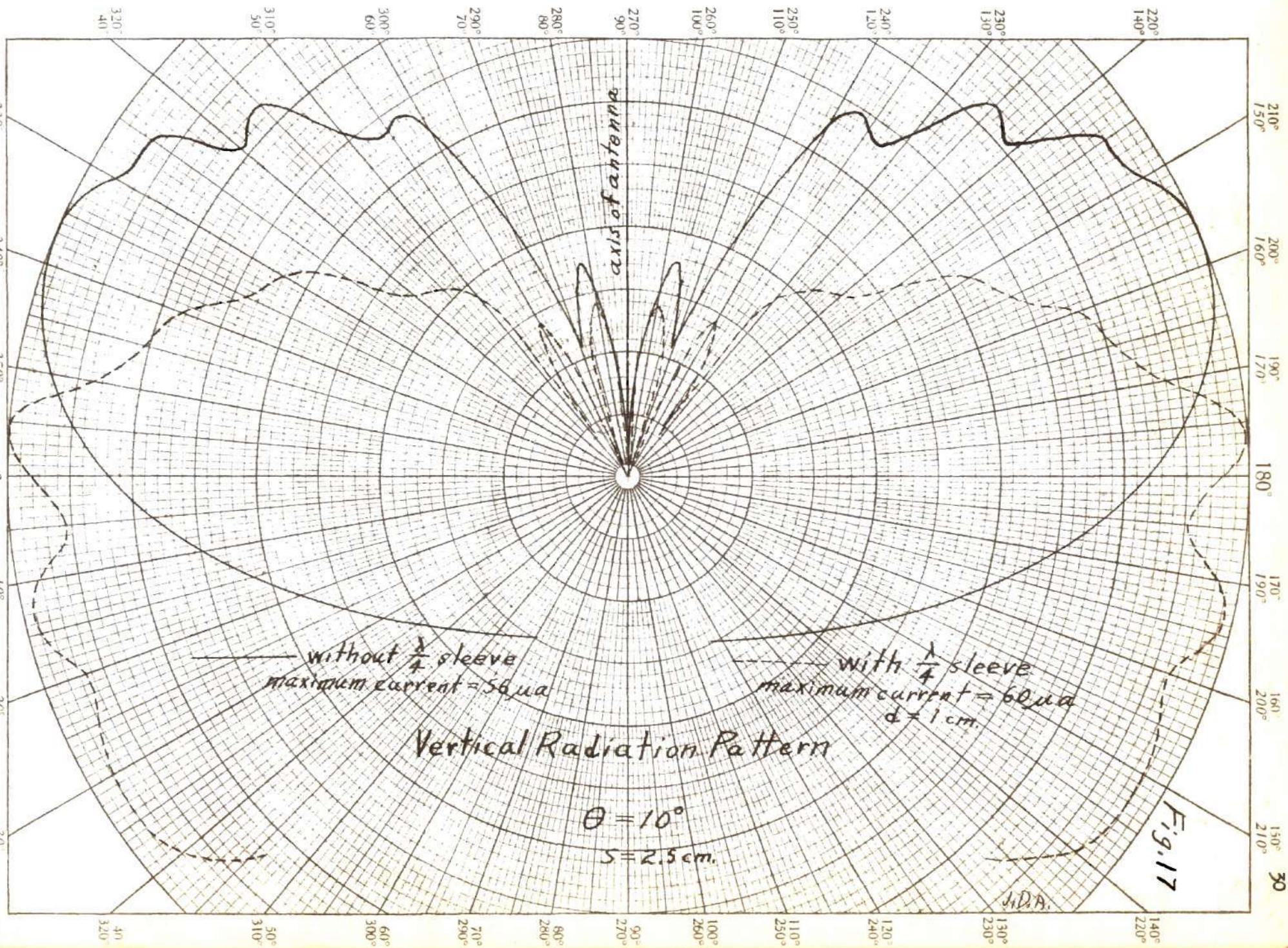
FIGURE 15
 Close Up of Cone Pairs
 Showing 70° cones with $s=7.4$ cm. and 10°, 20°, 30°, 40°, 50°, and 60° cones
 with $s=\frac{\lambda}{f}$

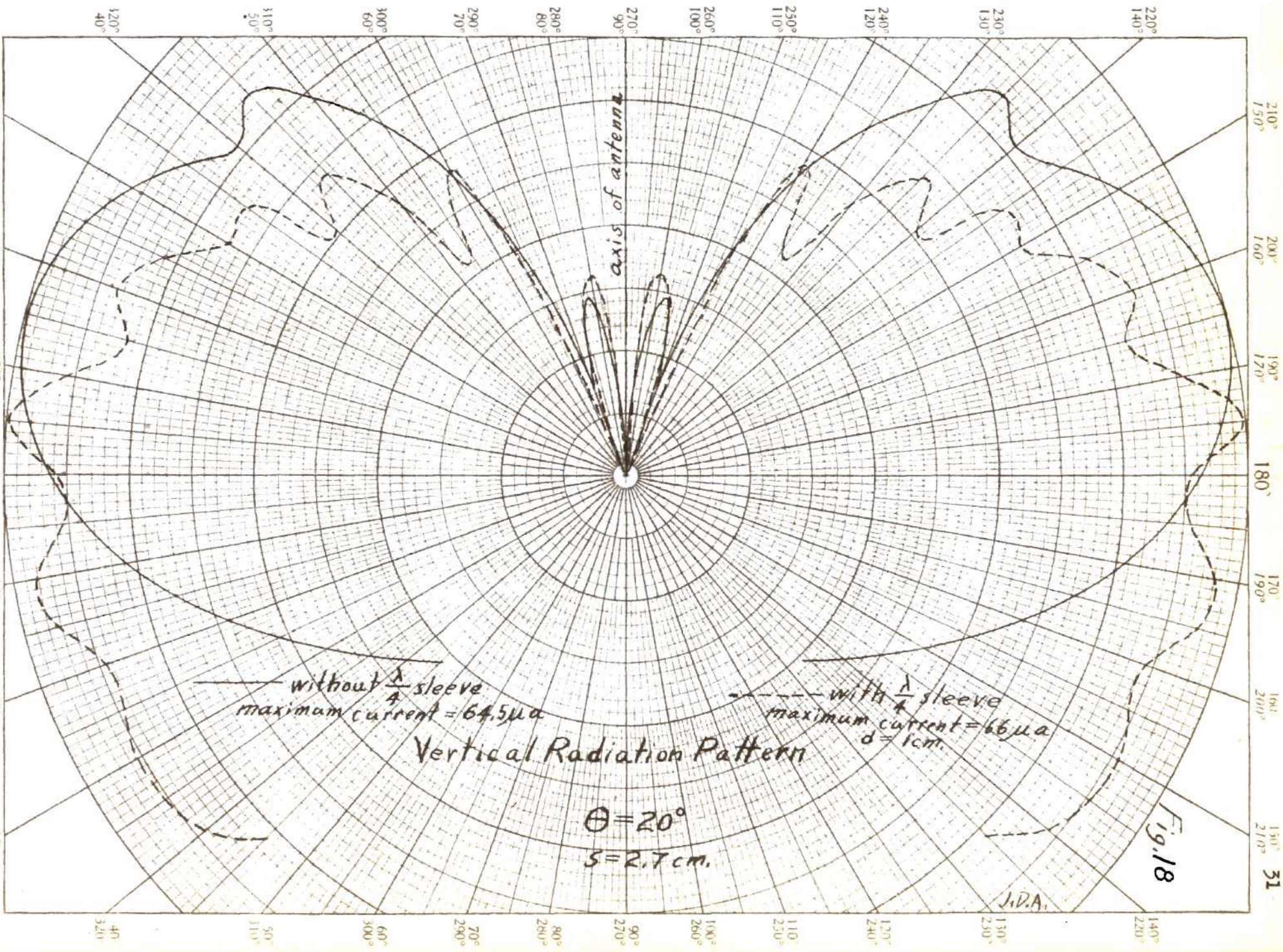
antenna parabola was then rotated slightly to obtain a maximum detector current reading. This orientation of the receiving antenna was not again changed. A measurement of detector current was made for the zero, or horizontal, position and for every five degrees of rotation as the slotted line mounting assembly was turned in a counterclockwise direction about its bearing. The rotation continued through 90° to a position where the receiving antenna was directly above the biconical horn antenna. The direction of rotation was then reversed and measurements were taken again at the same five degree points. The clockwise rotation continued beyond the horizontal to a position where the receiving antenna was 45° below. The slotted line mounting assembly was then turned back to the zero position again taking measurements of the detector current every five degrees along the way. By this process detector current was measured twice for every point between and including 45° below the horizontal with respect to the biconical antenna and 90° above. In some cases there was a difference of several microamperes in the detector current meter readings for the two measurements made at each position. This difference occurred mostly in the region where the back end of the slotted line was nearest the Klystron cabinet. In this position the flexible coaxial cable from the Klystron to the slotted line sagged in a U-shaped curve. In positions where the flexible cable was stretched out fairly straight, there was no difference in the two readings at a point. It is believed, therefore, that the flexure and twisting of the cable in the bent positions caused changes in the cable's attenuation resulting in differences in the two readings.

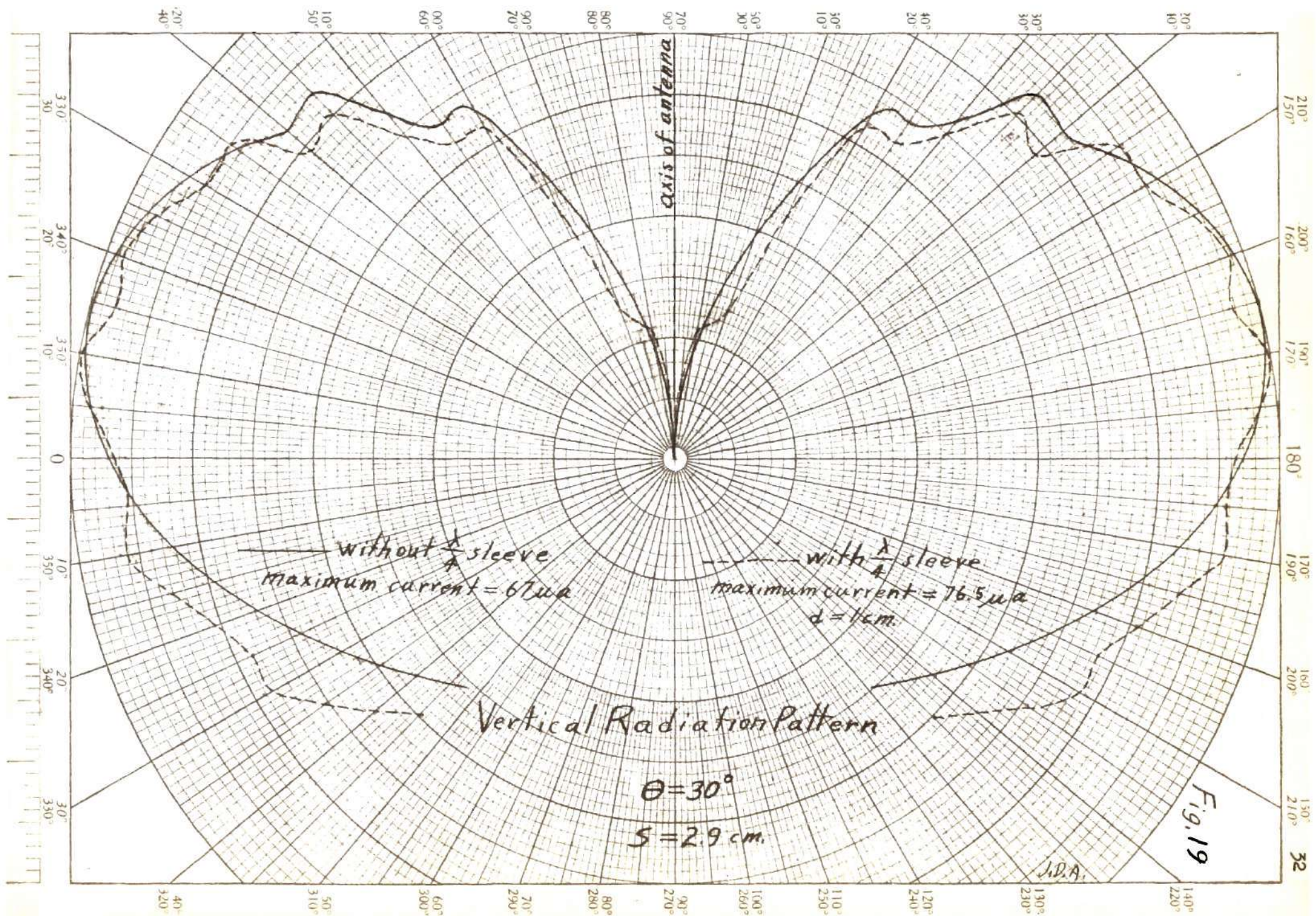
The average of the two readings was taken for making further calculations. Measurements were made on both sides of the position in which the receiving antenna was vertical to the biconical assembly. It was found that there was a variation for corresponding points of not more than $\pm 5\%$. Because of this small variation, the righthand side of the vertical radiation patterns is plotted as a mirror image of the lefthand side. However, before any radiation pattern could be plotted, all the measured data had to be corrected by the calibration curve of Fig. 11a. The angles measured from 0° on the lefthand edge of the radiation pattern sheet correspond to the angles made by the receiving antenna with respect to the biconical horn antenna.

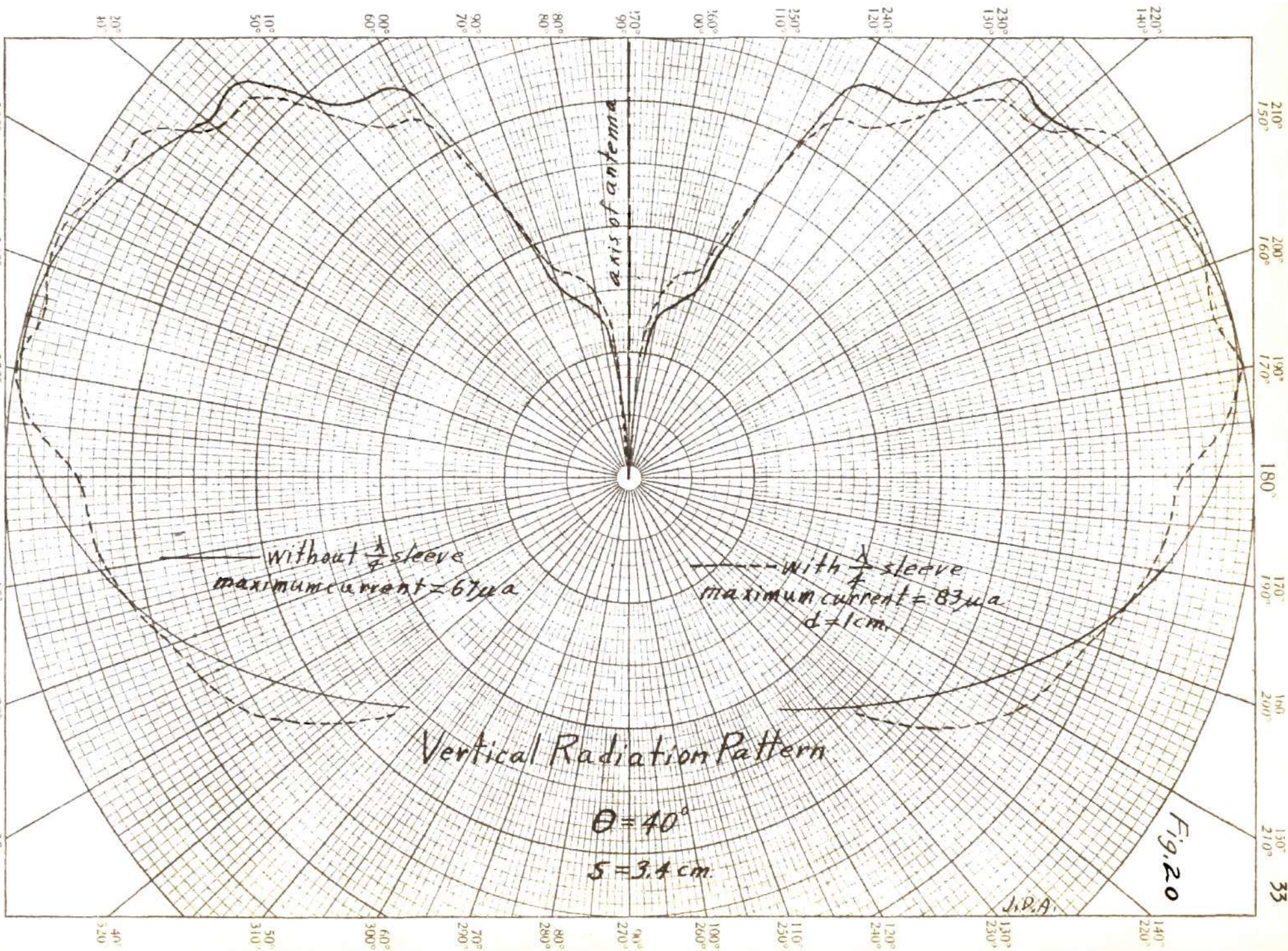
Measurements necessary to determine the input impedance of the antennas were made under all of the same conditions as the radiation patterns. The actual measurements were not mechanically different from that used to determine the calibration curves of the v.s.w.r. detector. In general, measurements were made only of the position and height of the maximum and minimum points along the sliding probe scale. In certain cases mentioned later, the standing wave intensity was measured over the full length of the line slot. As will also be shown later, the only data necessary to determine the input impedance of the biconical antennas is the v.s.w.r. and the shift in the position of the minimum point with respect to the position of the minimum when the line was short-circuited. The measured values of the maximum and minimum were corrected by the calibration curve of Fig. 9a before the voltage standing wave ratio r could be determined.

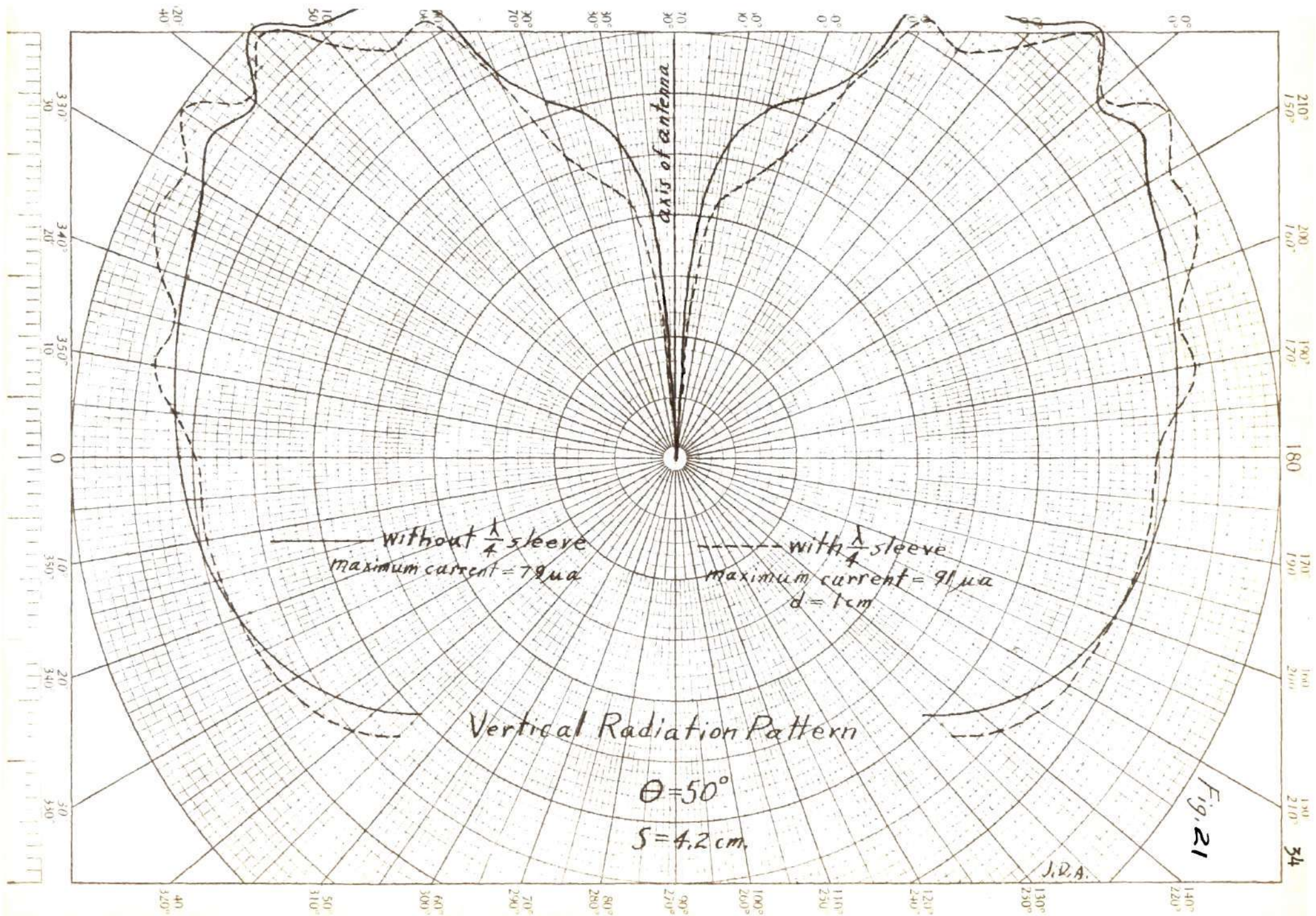


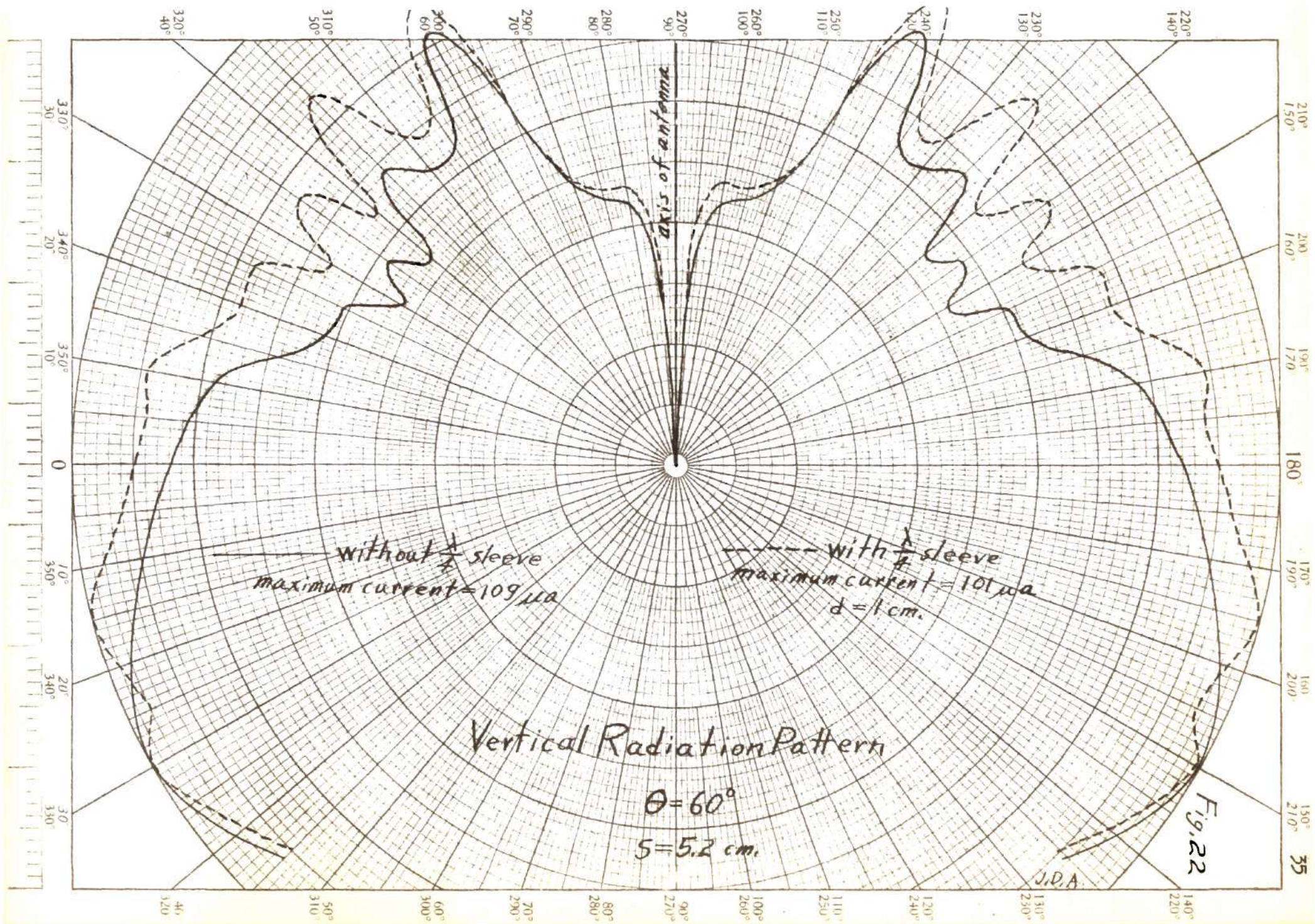


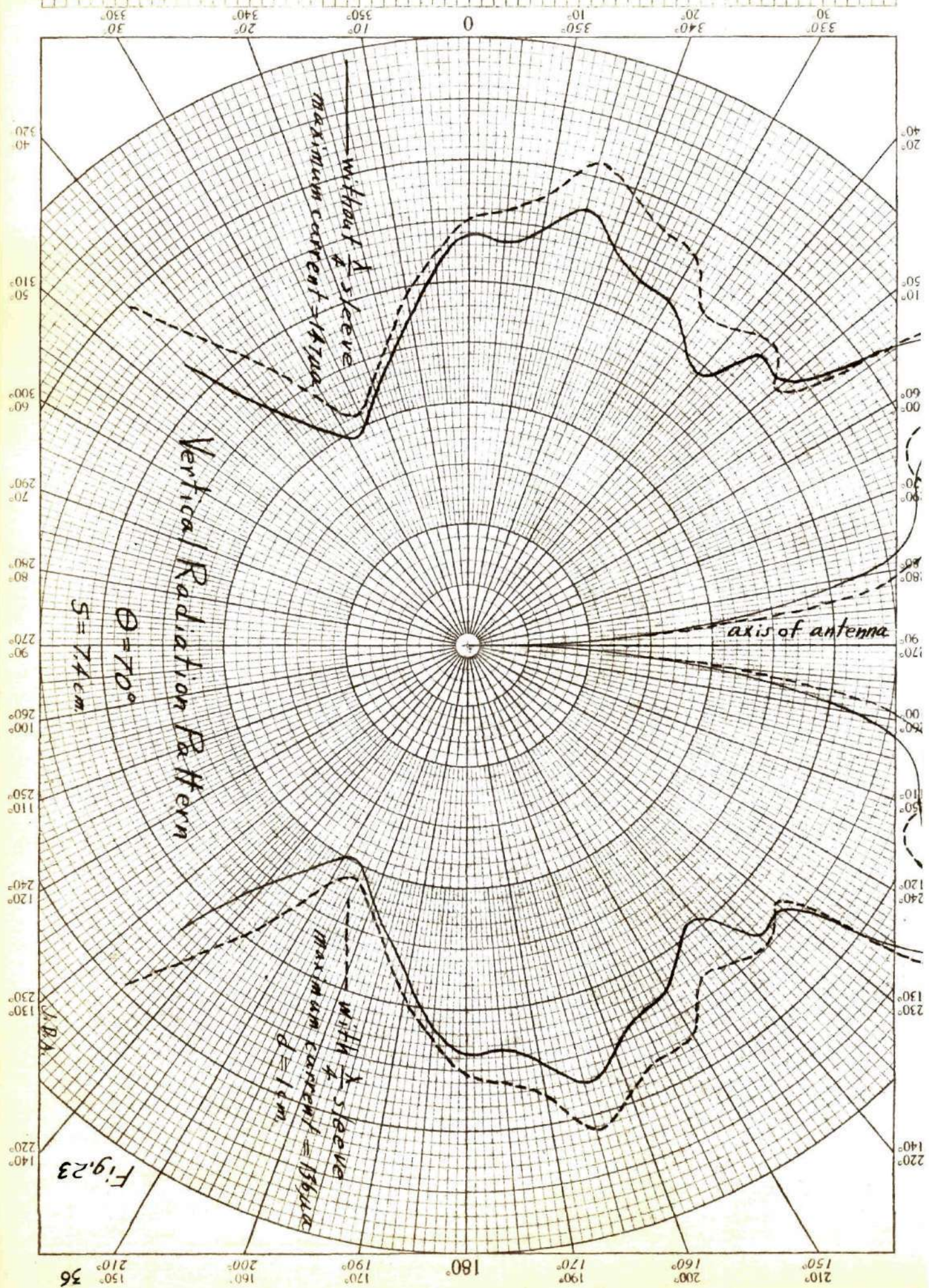












210°
150°

200°
160°

190°
170°

180°

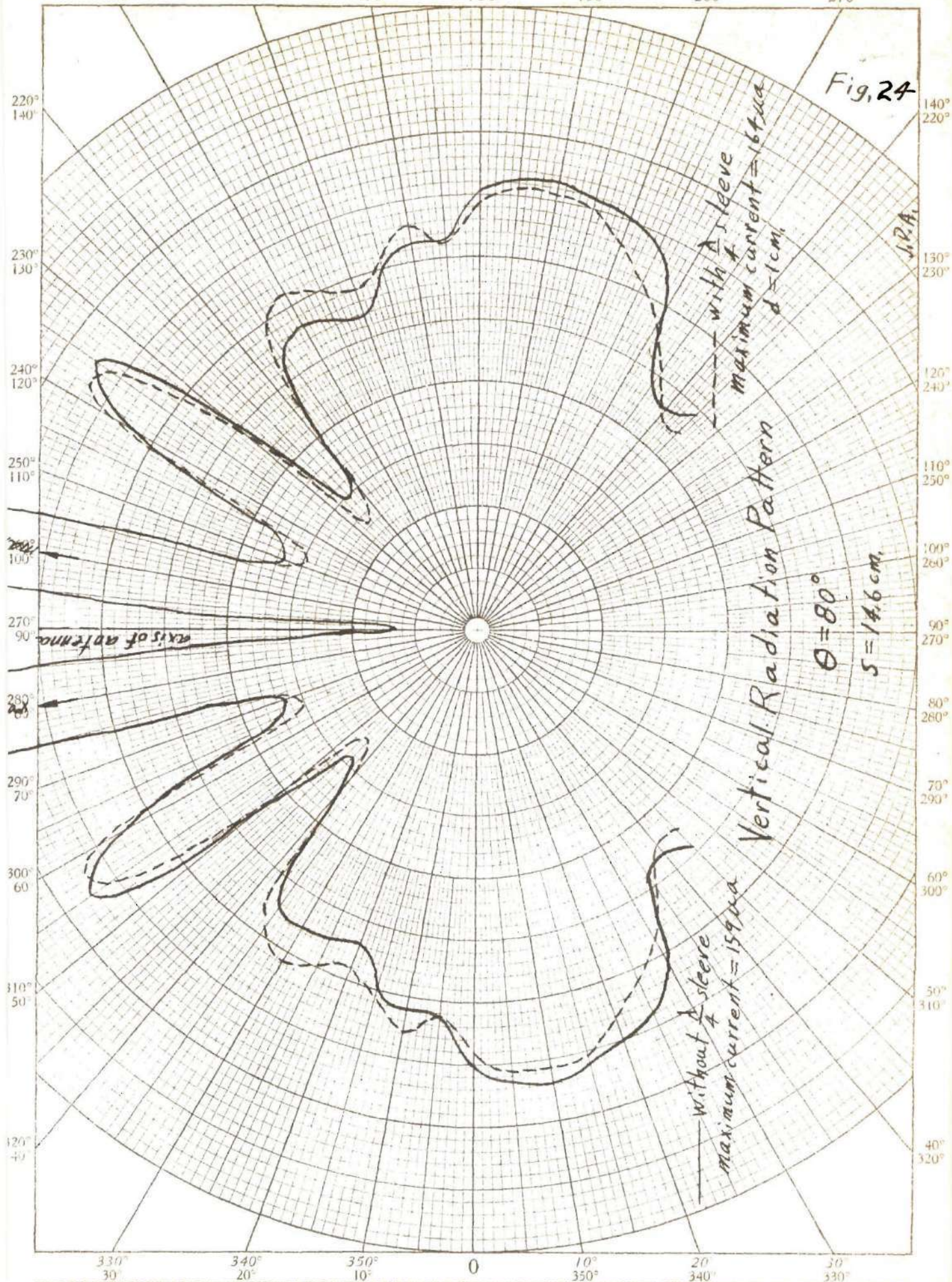
170°
190°

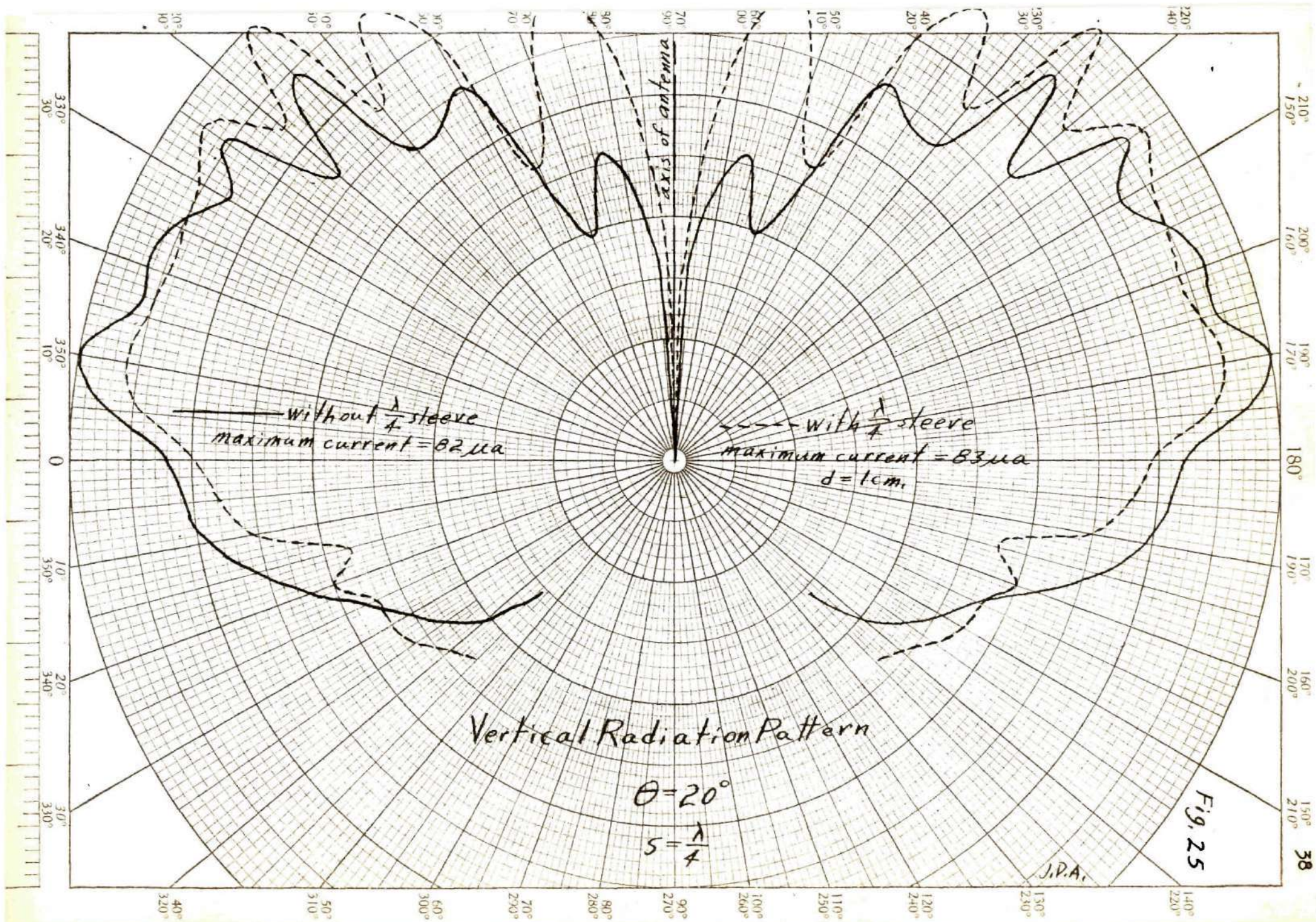
160°
200°

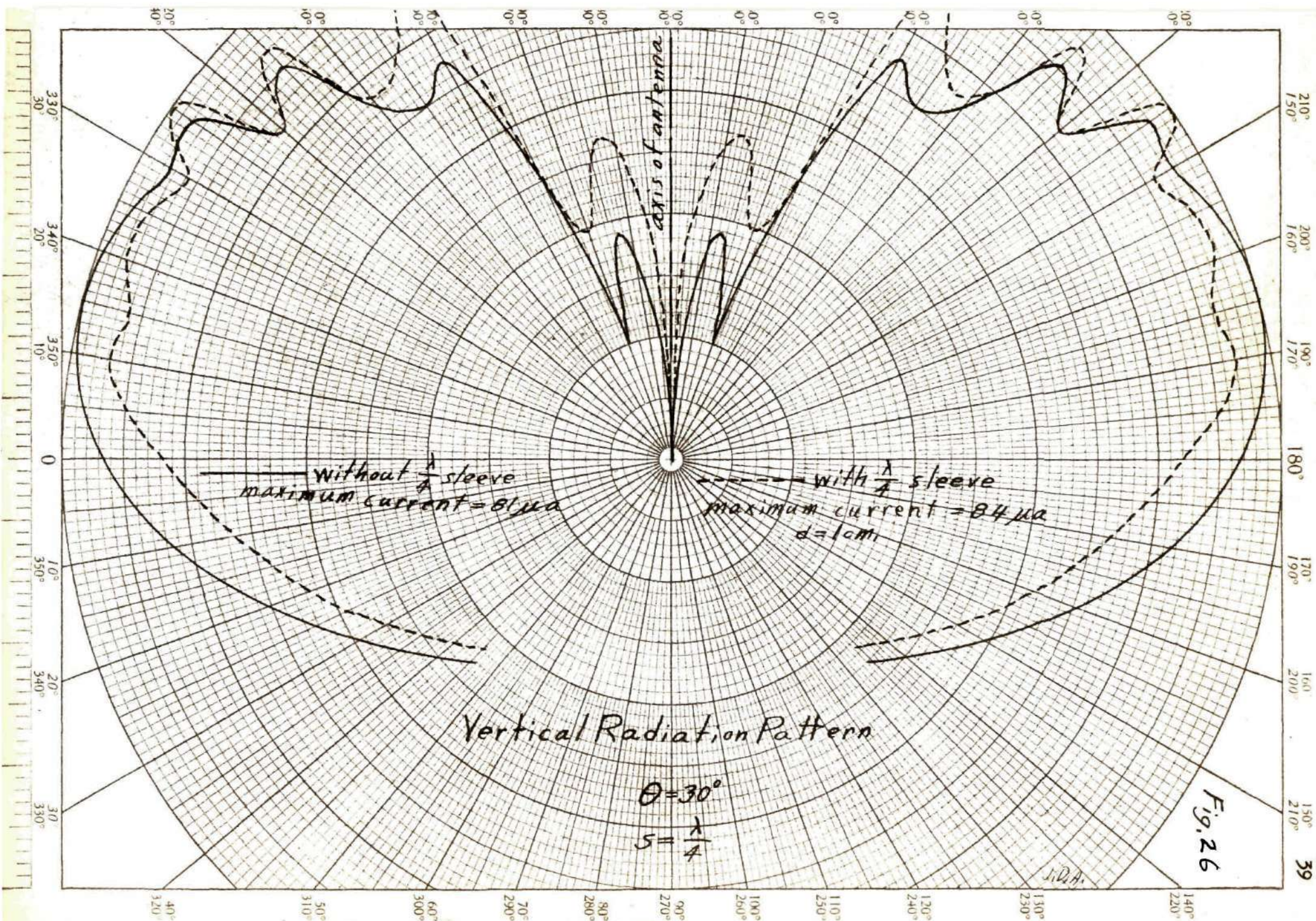
150°
210°

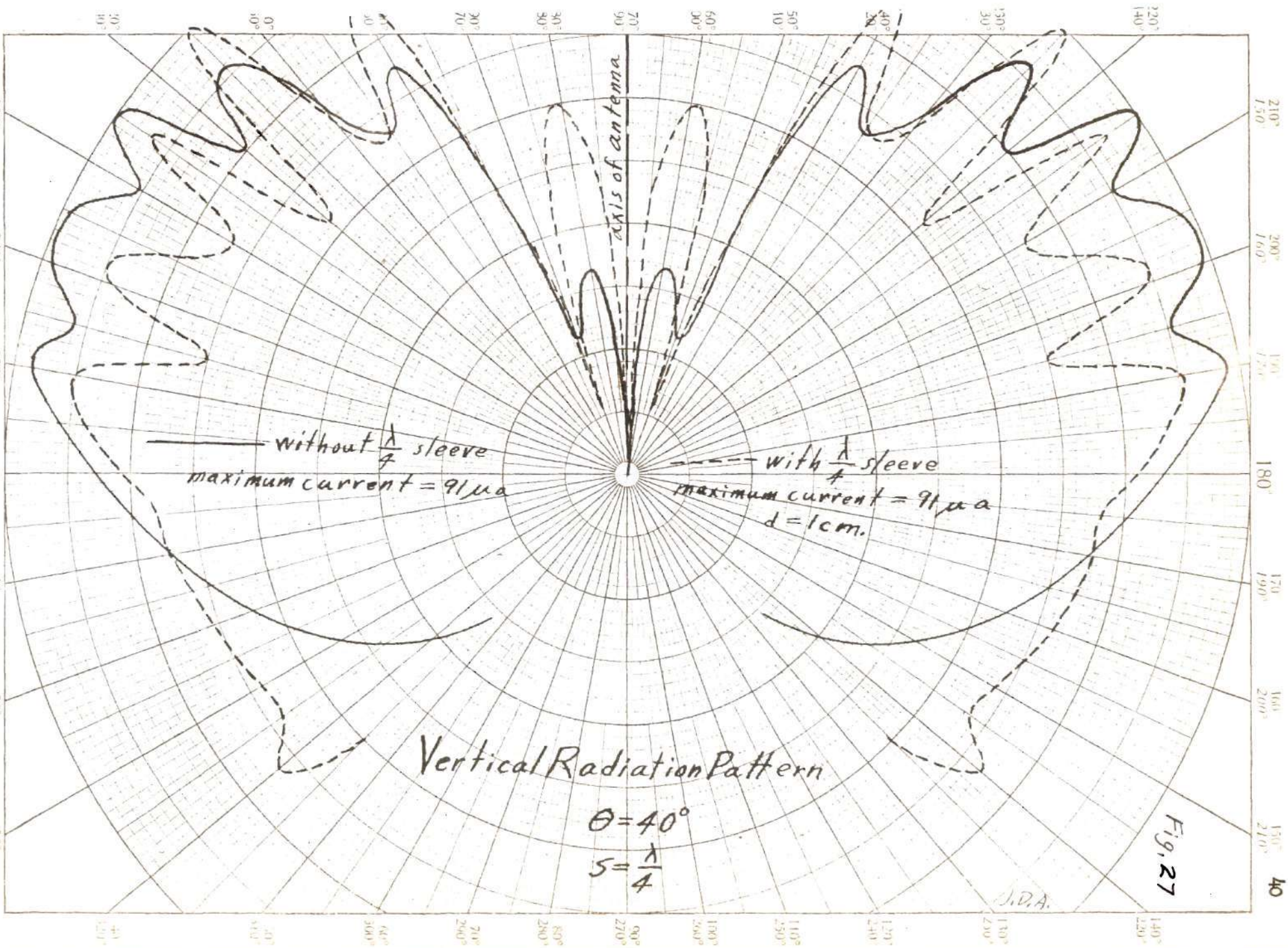
37

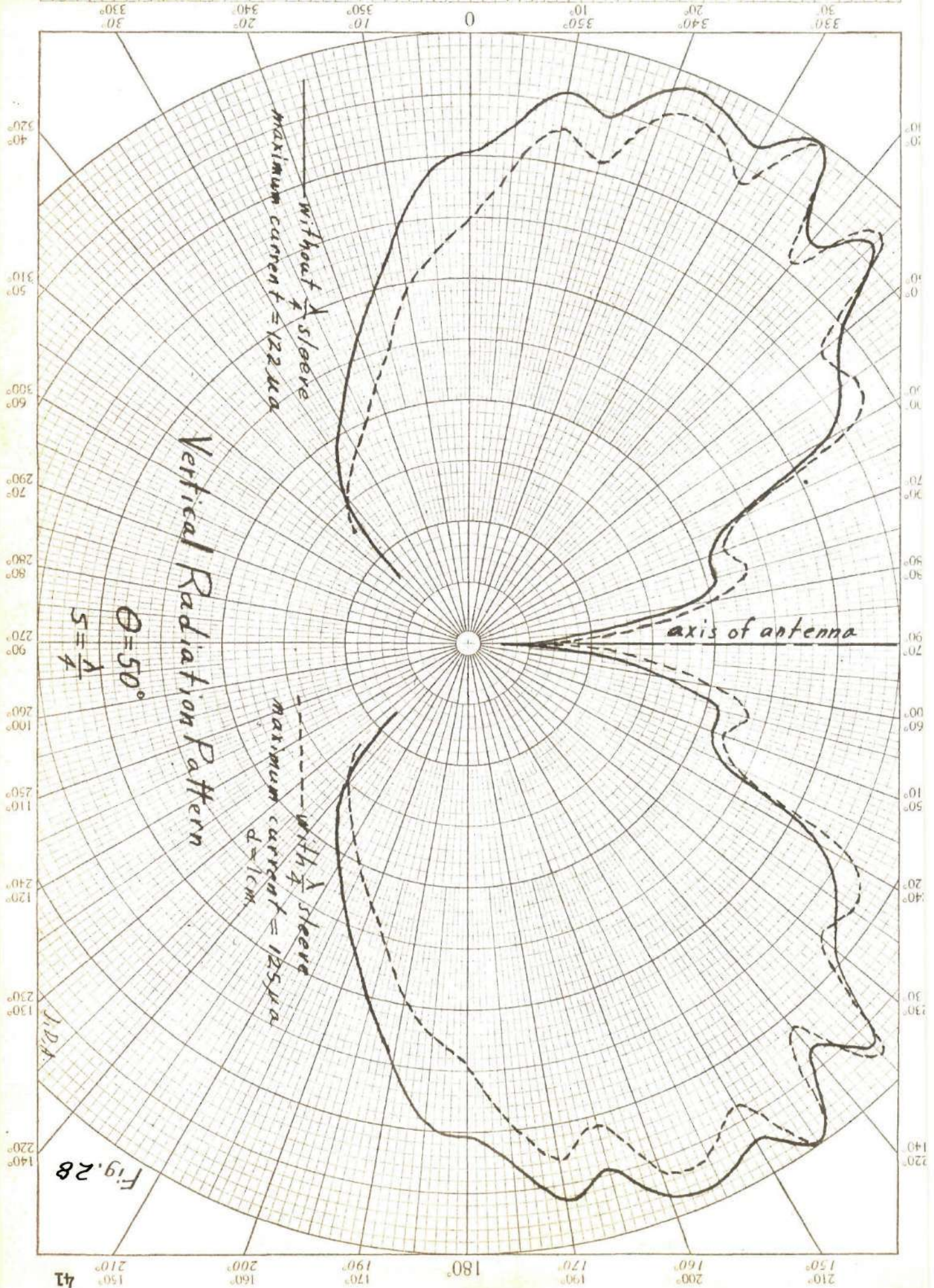
Fig. 24

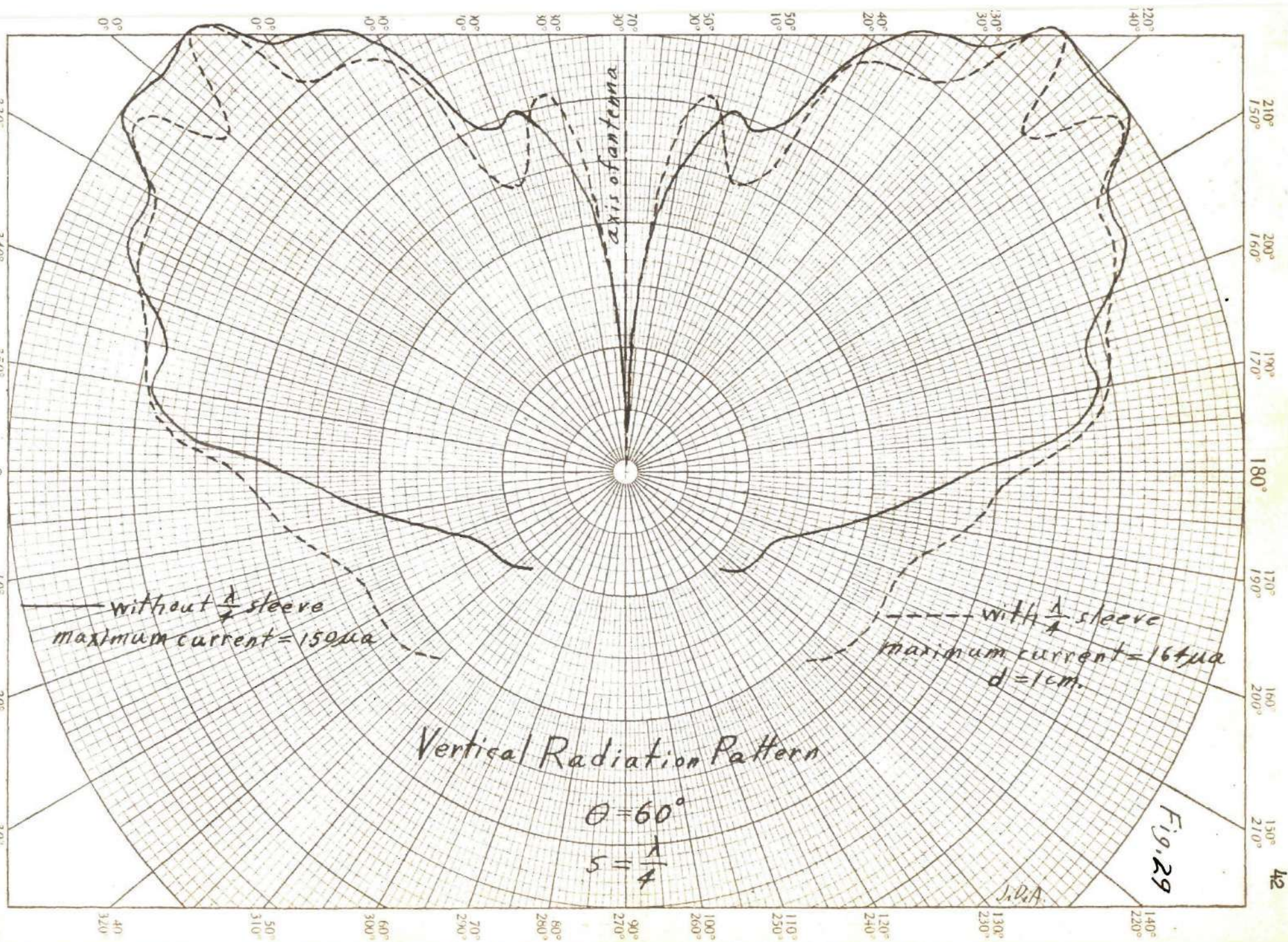


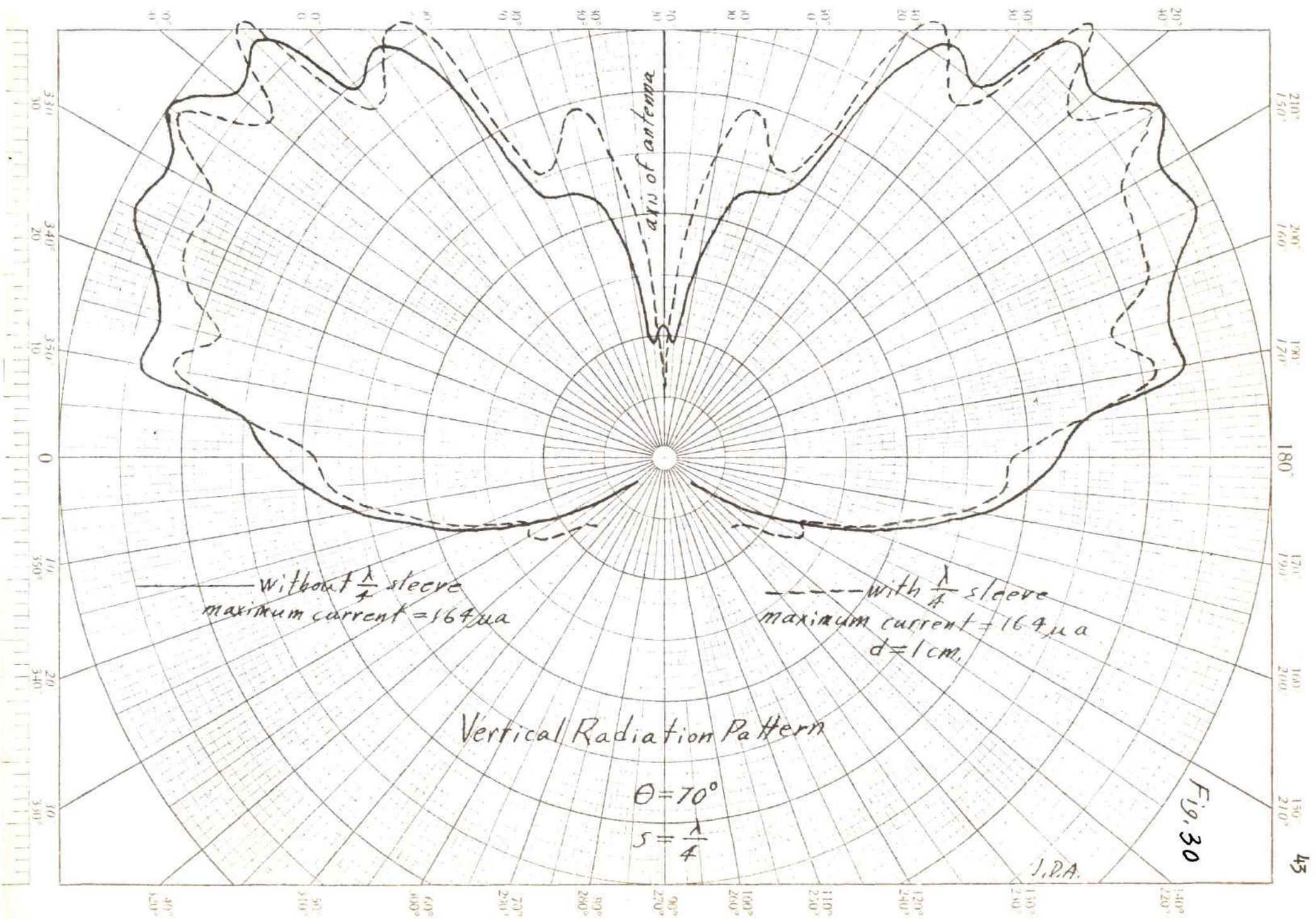


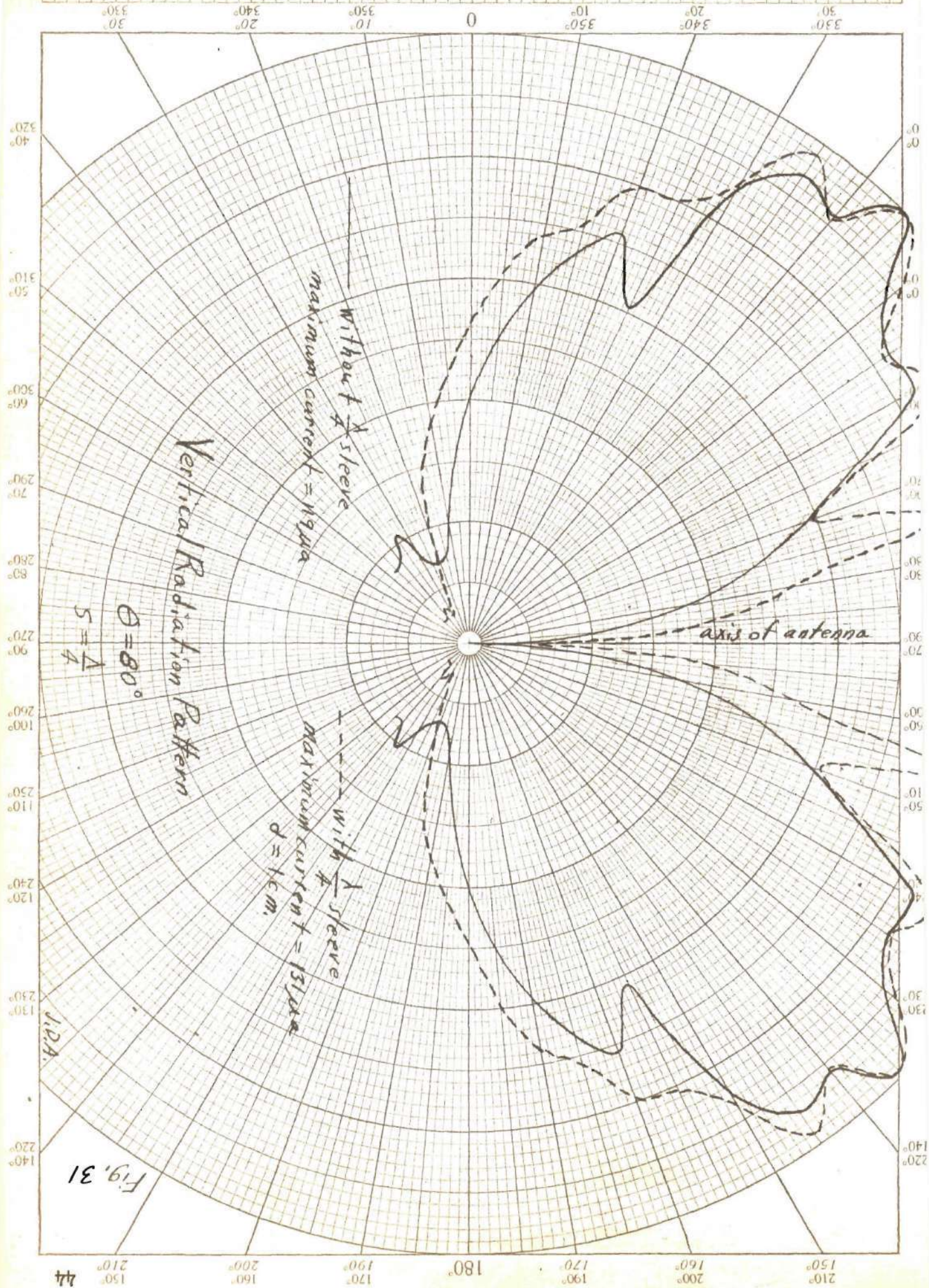












DISCUSSION OF RADIATION PATTERNS

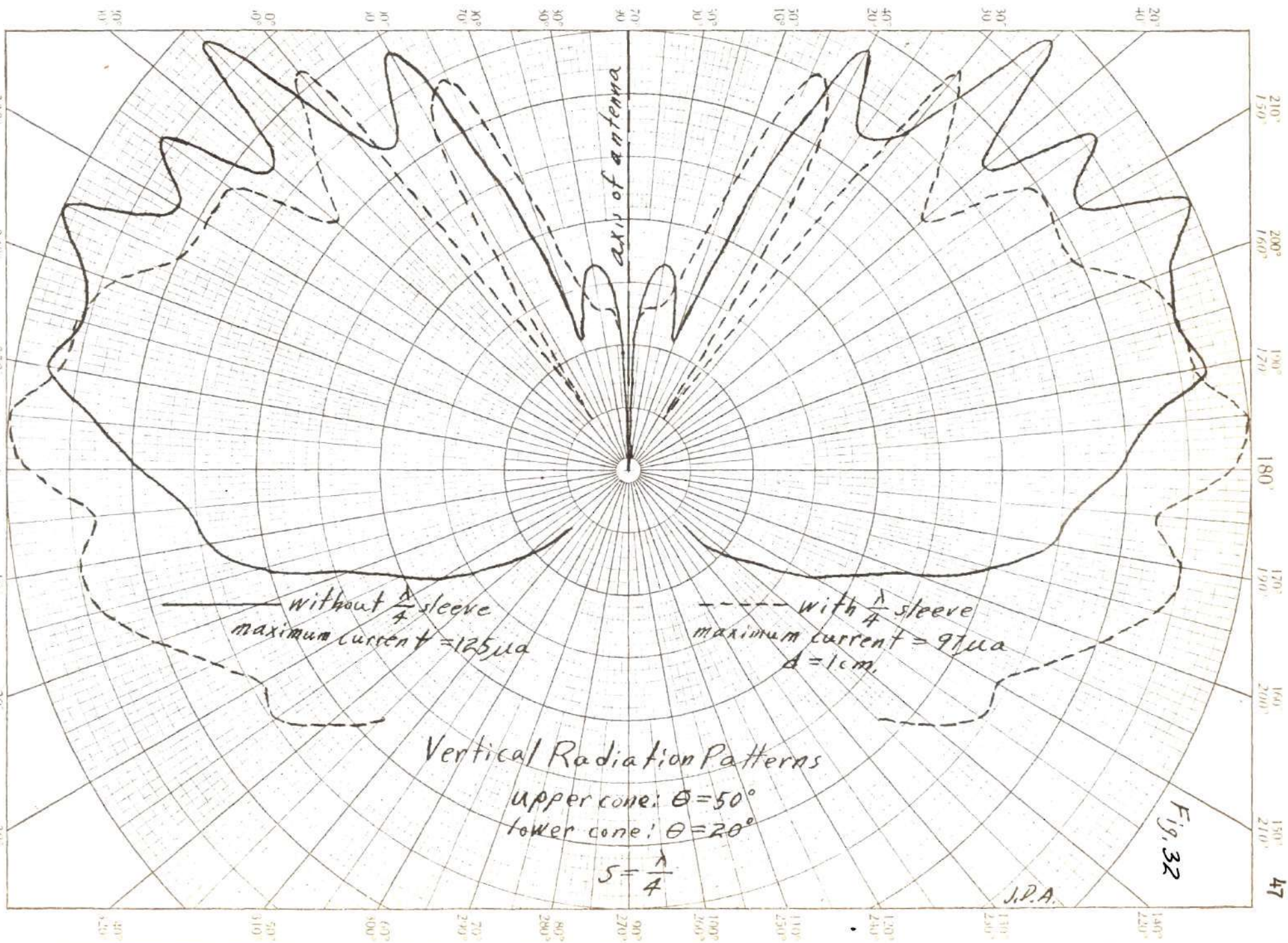
From an inspection of the radiation patterns on pages 29 to 44, it is evident that in addition to the major lobes there are many minor lobes produced by the antennas used in this work. On the other hand, all of the patterns show a greater distribution of energy in the horizontal plane than can be had with a half-wavelength coaxial dipole antenna.

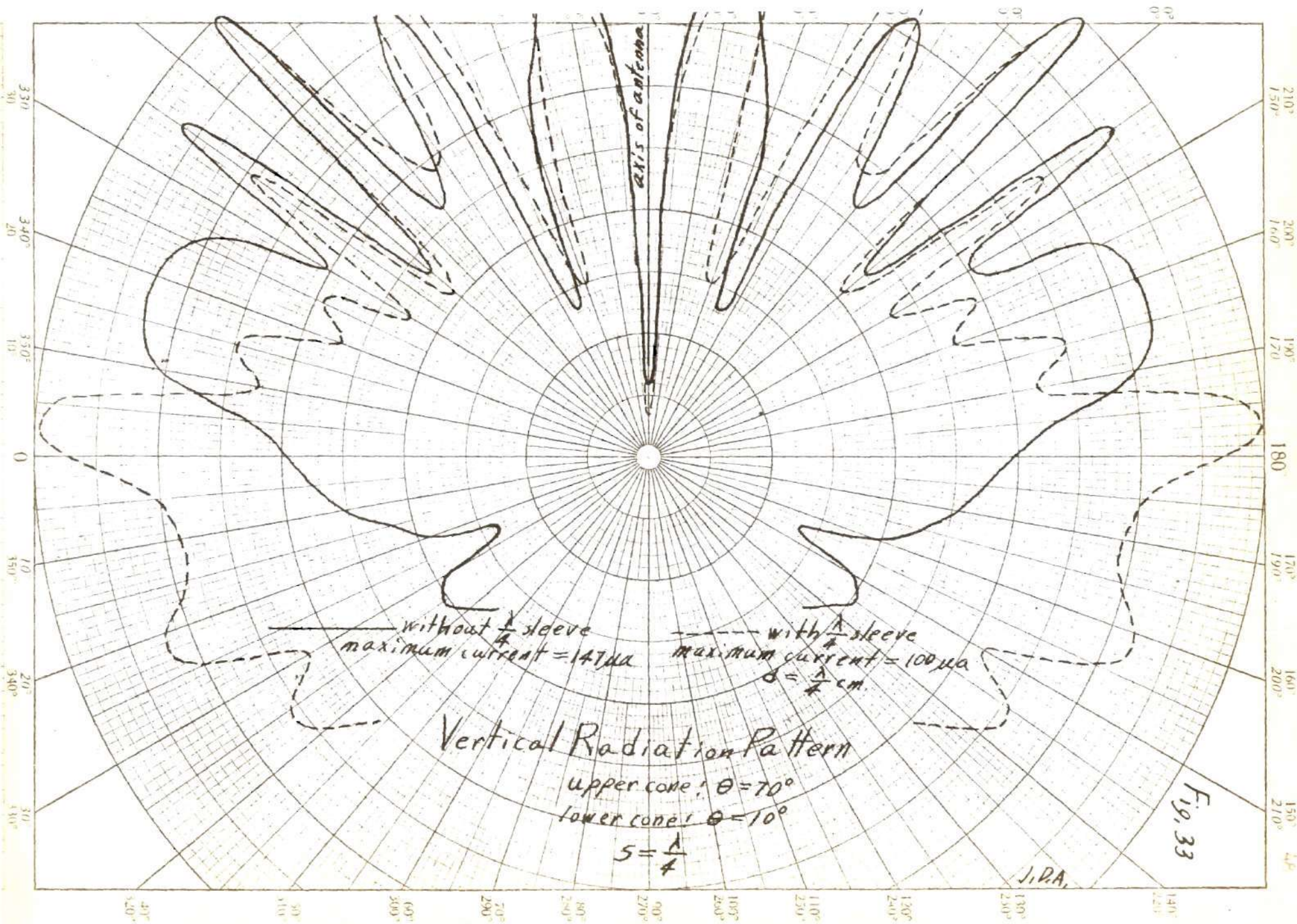
There are two other important characteristics to be noted in the radiation patterns. In the first place, almost without exception, there are many minor lobes superimposed on the major lobe. In many cases this effect seems to be increased by the addition of the detuning sleeve. The purpose of the detuning sleeve is to prevent antenna currents from flowing down the outside of the coaxial feed line and producing radiation which would distort the field produced by the actual antenna elements. While the detuning sleeve does have some definite advantages, it does not seem to have solved the problem of smoothing out the radiation patterns. This saw-tooth effect is very likely the result of improper spacing of the sleeve below the bottom cone of the antenna assembly. Because of the flare of the cones, the most effective distance can be located only by trial and error. The sleeve does have the advantage, in some cases, of causing the major lobes to be more nearly horizontal than they would be if no sleeve were used.

The second important characteristic to be noted is the tendency of all of the lobes to turn upward. This effect may be largely due to the fact that the outer diameter of the coaxial feed line is much

larger than the diameter of the inner conductor. This makes the base diameter of the bottom cone of a pair exceed the base diameter of the top cone by the difference in the outside diameters of the inner and outer conductors. Because of the small physical size of the cones used, this difference in diameters is a fairly large per cent of the base diameters of the cones and is very apparent when looking at them. See Figs. 13, 14, and 15. The jutting of the edge of the bottom cone beyond the edge of the top apparently produces radiation directed upward, which causes the whole radiation pattern to be angled upward. In an effort to make the lobes more nearly horizontal, two antennas were tried, with the top cone having a much larger angle of flare than the bottom one. The patterns produced by these two antennas are shown in Figs. 32 and 33 on pages 47 and 48. Obviously, there is little decrease in the upward tendency of the lobes, and in the case of the 70° - 10° antenna, a fairly large part of the energy is in the form of sharp minor lobes directed upward. There is also a large lobe directed almost horizontally as would be expected.

In Fig. 16 is shown the radiation patterns of a half-wavelength dipole antenna, with three positions of a $\frac{\lambda}{4}$ detuning sleeve. These patterns are extremely irregular for angles close to the vertical. In Figs. 17 to 24 on pages 30 to 37 are shown the patterns for cones whose slant height s increases approximately as the tangent of the angle of flare. From 10° to 50° the patterns are fairly smooth and show no large vertical lobes. The 60° , 70° , and 80° cones show increasingly large vertical lobes and a more irregular pattern in general. It is thought that this may be due to concentrations of charge on the outer face of the





top cone. These concentrations may, in turn, be due to concentric standing waves about the outer face of the top cone. The 70° cone was approximately 1.5λ across the base and, therefore, could support three maximum points of standing waves across its diameter. The 80° cone was approximately 3λ in base diameter and could, therefore, support six standing wave maxima. The field about the outer face of the 80° cone was probed with a half-wavelength center fed antenna and it appeared that these standing waves did actually exist.

When the antennas were cut down so that all had a slant height s of $\frac{\lambda}{4}$ it was found that there was little or no tendency to produce sharp vertical secondary lobes. See Figs. 25 to 31 on pages 38 to 44. The 10° cone with $s = \frac{\lambda}{4}$ produced a pattern which was not significantly different from Fig. 17 and, therefore, was not plotted. In these patterns the upward tendency of the lobes is very marked. It should be noted that the best overall pattern is obtained with the 70° cones. This antenna has an angle of opening between the cones of 40° . This value for the angle of opening compares favorably with the results obtained by Barrow and Lewis for rectangular horns,⁶ and by Southworth and King for circular horns.⁷

6. W. L. Barrow and F. D. Lewis, "The Sectoral Electromagnetic Horn," Proc. I. R. E., 27, 41, Jan., 1939.

7. G. C. Southworth and A. P. King, "Metal Horns as Directive Receivers of Ultra-Short Waves," Proc. I. R. E., 27, 95, Feb., 1939.

DISCUSSION OF INPUT IMPEDANCE

In making the v.s.w.r. measurements necessary to determine the input impedances of the antennas, it was noticed that the standing waves occurred along the slot in such a way that it was convenient to measure two minimum and one maximum point. It was further noticed that the minimum point nearest the load end of the line was always larger than the minimum point toward the generator end. A typical case is plotted in Fig. 34 on page 51. When the standing waves for the 80° cone with $s = 14.6$ cm. were measured no maximum or minimum points could be found, but the curve showed a definite upward trend toward the load end of the slot. See Fig. 35 on page 52. The fact that the curve showed no measurable maximum or minimum points indicates that the input impedance of the 80° cone is almost equal to the characteristic impedance of the line. As all of the standing wave measurements showed the same upward trend at the load end of the slot, it would seem that this is an inherent characteristic due to mechanical discrepancies in the line. In determining the v.s.w.r. the single maximum and small minimum points were used.

The input impedances of the biconical horn antennas are calculated in the same way as would be used in determining the value of any load impedance on a nondissipative transmission line. The input impedance of a transmission line of characteristic impedance Z_0 terminated in an arbitrary impedance Z is given by the general expression,

8. For development see W. L. Everitt, "Communication Engineering," p. 158, McGraw-Hill Book Co., N. Y., 1937, and L. A. Ware and H. R. Reed, "Communication Circuits," p. 73, John Wiley and Sons, N. Y., 1944.

Detector Current in μa (corrected)

260
240
220
200
180
160
140
130
120
100

Load
End

1 2 4 6 8 10 12 14 16 18 20 22 24 26 28 30 32 34

Scale Divisions on Slotted Line

Generator
End

Fig. 34

Standing Waves in Slotted Line

$\theta = 40^\circ$, $s = \frac{\lambda}{4}$, and $\frac{\lambda}{4}$ detuning sleeve, $d = 1 \text{ cm}$.

J.D.A.

Detector Current in μa (corrected)



Standing Waves in Slotted Line

$\theta = 80^\circ$, $s = 14.6\text{ cm.}$

J.D.A.

$$Z_{input} = Z_o \left[\frac{Z \cosh \gamma l + Z_o \sinh \gamma l}{Z_o \cosh \gamma l + Z \sinh \gamma l} \right]. \quad (1)$$

Where γ is the propagation constant and

$$\gamma = \alpha + j\beta. \quad (2)$$

If we assume that the line is dissipationless, we may set α , the attenuation constant, equal to zero. This leaves

$$\gamma = j\beta. \quad (3)$$

Substituting back in Eq. 1, we get

$$Z_{input} = Z_o \left[\frac{Z \cos \beta l + j Z_o \sin \beta l}{Z_o \cos \beta l + j Z \sin \beta l} \right]. \quad (4)$$

Dividing numerator and denominator by $\cos \beta l$, we get

$$Z_{input} = Z_o \left[\frac{Z + j Z_o \tan \beta l}{Z_o + j Z \tan \beta l} \right]. \quad (5)$$

If E_{min} , the voltage standing wave minimum, occurs at the load, then the load must be a pure resistance equal to $\frac{Z_o}{r}$ where r is the measured ratio

$$r = \frac{|E_{max}|}{|E_{min}|}. \quad (6)$$

The input impedance of a point of E_{min} is then $\frac{Z_o}{r}$. If we take l as the distance of the shift in the minimum point from a minimum when the line is shorted, we may write,

$$\frac{Z_o}{r} = Z_o \left[\frac{Z + j Z_o \tan \beta l}{Z_o + j Z \tan \beta l} \right]. \quad (7)$$

Solving for Z , we get

$$Z = Z_o \left[\frac{1 - j r \tan \beta l}{r - j \tan \beta l} \right]. \quad (8)$$

However,

$$\beta l = \frac{2\pi l}{\lambda} \quad (9)$$

where $\lambda = 9.920$ cm. and $l = 0.1$ inch, or 0.254 cm. As was said, the probe motion was measured in 0.1 inch units, so to find the angular value of βl , we may set

$$\begin{aligned} \beta l &= \frac{n(360)(0.254)}{9.920} \\ &= n(9.08) \quad \text{degrees} \end{aligned} \quad (10)$$

9. R. W. P. King, H. R. Mimno, and A. H. Wing, "Transmission Lines, Antennas, and Wave Guides," pp. 40-41, McGraw-Hill Book Company, New York, 1945.

where n is the number of probe scale units moved from the voltage node position when the line was shorted to the nearest minimum point when an antenna was in place. To maintain the correct sign of the load impedance, or the input impedance of the antenna, the angle βl must be minus when the shift is toward the load end of the line and plus when the shift is toward the generator end. This is because an inductive reactance, having a positive angle, produces a shift in the minimum point toward the load end and, therefore, requires a negative sign before βl to produce a positive angle in the value of Z as found from Eq. 8. The opposite is true of a capacitive reactance. The same results as obtained from Eq. 8 may also be had from curves plotted in a manner similar to the standard transmission line circle diagrams.¹⁰

Before the above information can be applied, the characteristic impedance and dissipationless character of the slotted line must be determined. The characteristic impedance of a coaxial transmission line is given by:¹¹

$$Z_0 = \frac{1}{2\pi} \sqrt{\frac{\mu}{\epsilon}} \ln \frac{b}{a} \quad \text{ohms} \quad (11)$$

10. F. E. Terman, "Radio Engineers' Handbook," p. 180, McGraw Hill Book Co., N. Y., 1945, and J. R. Meagher and H. J. Markley, "Practical Analysis of Ultra High Frequency," pp. 20-22, (booklet), R. C. A. Service Co., Camden, N. J., 1943.

11. R. I. Sarbacher and W. A. Edson, "Hyper and Ultrahigh Frequency Engineering," p. 281, John Wiley & Sons, N. Y., 1943, and L. A. Ware and H. R. Reed, op. cit. p 261.

where μ and ϵ are the permeability and dielectric constant of the space between the inner and outer conductors. The polystyrene spacing washers form only a very small part of the total dielectric and as the power factor in the wavelength region used is about 0.00070% and the dielectric constant is about 2.45, we may assume the dielectric of the slotted line to be effectively that of air or free space. On this assumption

$$\sqrt{\frac{\mu}{\epsilon}} = 120\pi \quad (12)$$

so

$$Z_0 = 60 \ln \frac{b}{a} \quad (13)$$

Now, the inner diameter of the outer conductor b for the small $3/8$ inch line is 0.313 inches and the outer diameter of the inner conductor a is 0.125 inches. This gives $Z_0 = 55.2$ ohms.

The values of the input impedance for all the antennas used in this work are tabulated in the Appendix on page 66. As can be seen, the impedances are mostly capacitive and less in absolute value than the Z_0 of the feed line. The 70° antenna with $s = 7.4$ cm. has an impedance almost the same as the line impedance and with only a small capacitive component. The 80° antenna with $s = 14.6$ cm., as was said, had no measurable v.s.w.r.; and, therefore, it is concluded that it matched

12. C. R. Englund, "Dielectric Constants and Power Factors at Centimeter Wavelengths," Bell System Technical Journal, 114, January, 1944.

the line very closely.

If the biconical system of Fig. 12 is thought of as a transmission line as mentioned in the Introduction, a characteristic impedance may be developed for it.¹³ This impedance is:

$$Z_o = \sqrt{\frac{\mu}{\epsilon}} \frac{1}{2\pi} \ln \left(\tan \frac{\theta_2}{2} \cot \frac{\theta_1}{2} \right) \quad (14)$$

where θ_1 and θ_2 are measured as in Fig. 12. When $\pi - \theta_2 = \theta_1$, Eq. 14 reduces to

$$Z_o = \sqrt{\frac{\mu}{\epsilon}} \frac{1}{\pi} \ln \cot \frac{\theta_1}{2} \quad (15)$$

Substituting for the value of $\sqrt{\frac{\mu}{\epsilon}}$ from Eq. 12

$$Z_o = 120 \ln \cot \frac{\theta_1}{2} \quad (16)$$

This equation is plotted in Fig. 36 on page 58.

An equivalent circuit has been developed for the biconical antenna which enables us to determine its input impedance from the antenna's geometry.¹⁴ The input impedance of the equivalent circuit shown in Fig. 37b may be found if the load impedance Z_L is known.

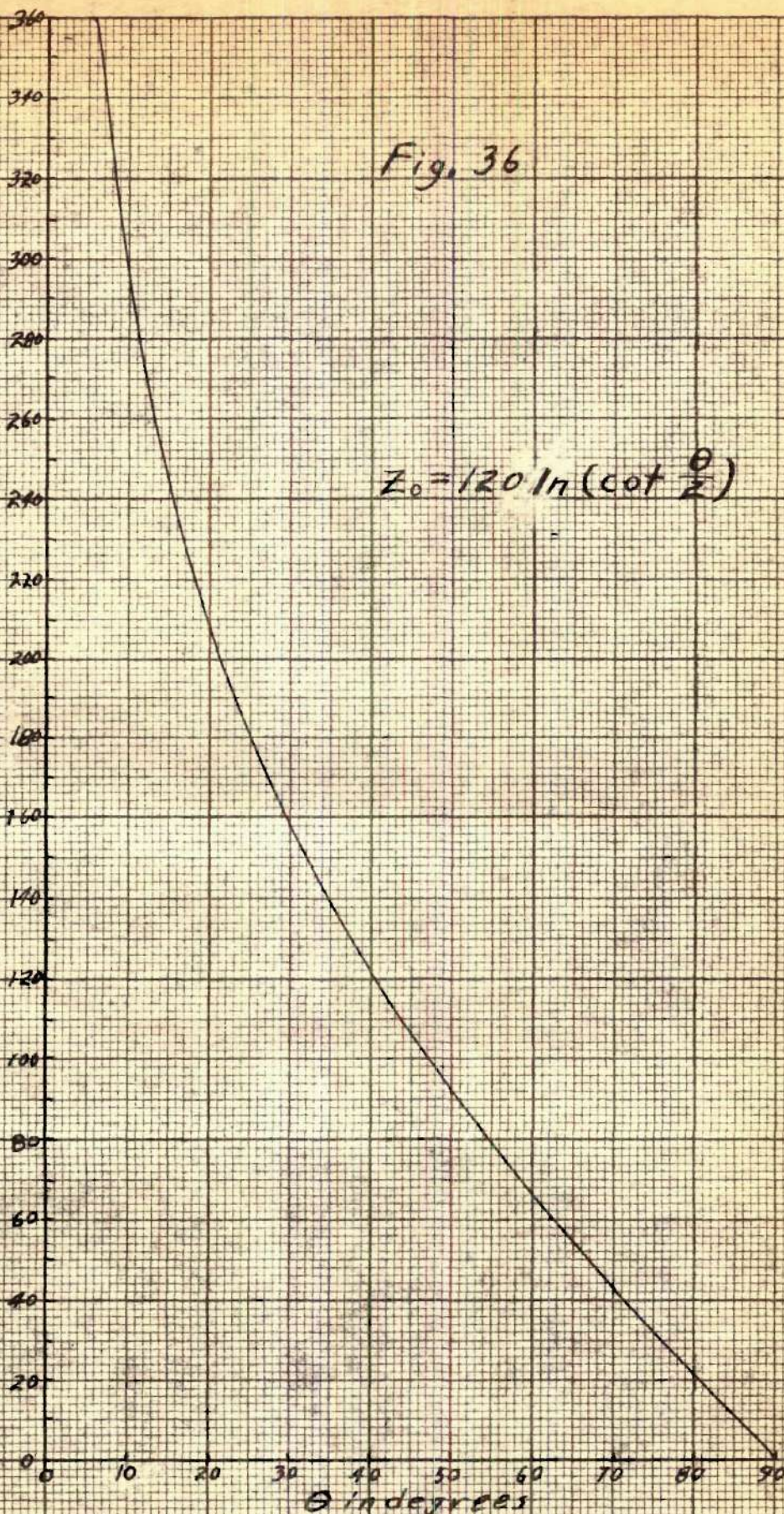
13. Slater, J. C., op. cit., pp. 202-205, and E. Weber, "Principles of Short Wave Radiation," Electronic Industries, February, 1943.

14. Ramo, S. and Whinnery, J. R., op. cit., pp. 482-489.

Fig. 36

$$Z_0 = 120 \ln \left(\cot \frac{\theta}{2} \right)$$

Z_0 in Ohms



Characteristic Impedance of Biconical Horn Antennas
plotted against angle of flare

H.P.A.

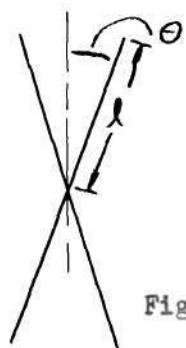


Fig. 37a

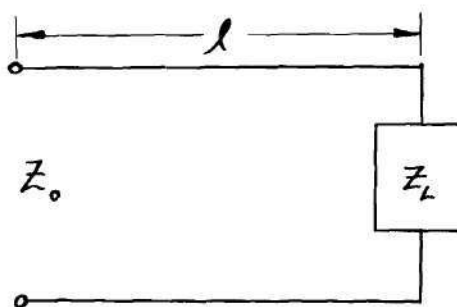


Fig. 37b

The value of Z_L is given by

$$Z_L = \frac{Z_0^2}{G(kl) + jF(kl)} \quad (17)$$

where Z_0 here is the value from Eq. 16 and $G(kl)$ and $F(kl)$ are defined

as

$$G(kl) = \sum_{m=0}^{\infty} b_m J_{2m+\frac{3}{2}}^2(kl) \quad (18)$$

$$F(kl) = -\sum_{m=0}^{\infty} b_m J_{2m+\frac{3}{2}}(kl) N_{2m+\frac{3}{2}}(kl) \quad (19)$$

where

$$b_m = \frac{30\pi kl (4m+3)}{(m+1)(2m+1)} \quad (20)$$

where also

$$kl = \frac{2\pi l}{\lambda} \quad (21)$$

and ℓ is the slant height of the cone as shown in Fig. 37a. This method was not used to make calculations in this paper because values of the Bessel function of the second kind of variable order and argument ($N_p(x)$) could not be found. However, judging from the curves in Ramo and Whinnery, it would seem that the measured values of input impedance tabulated in the Appendix are not far from the theoretical values as determined by the above method.

CONCLUSIONS AND RECOMMENDATIONS

The general results obtained in this work indicate that despite the fact that the short antennas produce patterns far less desirable than those produced by antennas having a long slant height, they still give more gain in the horizontal plane than can be obtained with a coaxial dipole antenna.

If the short biconical antennas were built on a larger scale, many of the imperfections already noted in the 10 centimeter models would disappear. In the first place, the outer diameter of the coaxial feed line would be a much smaller per cent of the cone's base diameter. The cones will then approach more closely the theoretically perfect set of Fig. 12. The physical structure can also be improved and better mechanical connections to the feed line can be obtained. In an effort to lower the upward-pointing major lobe, antennas with a large top flare were used. In the limit, the top cone would become a flat plane and the antenna would become one of the discone type.¹⁵ It is interesting to note that at the high end of the frequency band used by Kandoian, the discone's lobes also began to turn up. It would appear that the biconical horn antenna might also very well be used for broadcast purposes with frequencies as low as 100 megacycles. At higher frequencies, the physical size of the antenna may be reduced, or a larger ratio of slant height to wavelength may be used with corresponding increase in beam directivity. However, for any wavelength there is an optimum slant

15. A. G. Kandoian, "Three New Antenna Types and Their Applications," Proc. I. R. E., Feb., 1946.

height which should be used if it does not require too large an antenna.

The experimental work described in this paper was conducted in a room of approximately 18 by 30 feet. It is suspected that some of the small lobes causing the scalloped effect on the radiation patterns may be due to reflections from the walls of the room. Further work should, therefore, be conducted in a very large room or, better still, out in the open on some elevated structure. If a room is necessary, reflections may be reduced by covering the walls and ceiling with resistance cloth of about 377 ohms per square.

While the apparatus used in this work lacked refinement, it does have the advantage of being quite versatile. With the assembly of Fig. 1, almost any type of antenna scaled down for operation at 10 cm. may be tested. There is a multitude of improvements that may be made on the apparatus to increase its accuracy and ease of operation. One of the first things to be done would be to redesign the sliding probe carriage for smoother and more stable operation. The apparent discrepancies between the input impedances as tabulated in the Appendix and the values calculated from the equivalent circuit of Fig. 37b are very likely due to errors in measuring the v.s.w.r. It is to be noted, furthermore, that very accurate measurements of the v.s.w.r. can be had only with sliding probes of extremely precise mechanical construction. The second thing would be to redesign the end connections of the 3/8 inch line where the antennas are mounted so that an antenna may be built as a complete

16. Barrow, W. L., Chu, L. J., and Jansen, J. J., op. cit.

unit and slipped on and off the line with ease. The crystal detector assembly should also be redesigned to allow greater ease in changing the crystal.

In recording a large volume of data, as in this work, it would be very convenient to have a sensitive recording d.c. meter preceded by a d.c. amplifier with an amplitude response such as to compensate for the nonlinear crystal so that the recording meter's readings may be linear. An angular positioning system may also be added, which would be of a great convenience. Many complex radiation pattern recording systems have been developed, but it would not require much additional equipment to reduce to a great extent the drudgery involved in this
17
work.

BIBLIOGRAPHY

- Barrow, W. L., L. J. Chu, and J. J. Jansen, "Biconical Electromagnetic Horns," Proceedings of the Institute of Radio Engineers, 27, 769, December, 1939.
- _____, and F. D. Lewis, "The Sectorial Electromagnetic Horn," Proceedings of the Institute of Radio Engineers, 27, 41, January, 1939.
- Englund, C. R., "Dielectric Constants and Power Factors at Centimeter Wavelengths," Bell System Technical Journal, 114, January, 1944.
- Everitt, W. L., "Communication Engineering," McGraw-Hill Book Company, New York, 1937.
- Kandoian, A. G., "Three New Antenna Types and Their Applications," Proceedings of the Institute of Radio Engineers, February, 1946.
- King, R. W. P., H. R. Mimno, and A. H. Wing, "Transmission Lines, Antennas, and Wave Guides," McGraw-Hill Book Company, New York, 1945.
- Meagher, J. R., and H. J. Markley, "Practical Analysis of Ultra High Frequency," R. C. A. Service Company, Camden, New Jersey, 1943.
- Massachusetts Institute of Technology Radiation Laboratory Report, 263 (54-15), "Horizontally Polarized, 9.1 cm. Biconical Horn Beacon Antenna,"
- Massachusetts Institute of Technology Radiation Laboratory Report, 601-4, "Automatic Antenna Pattern Recorder."
- Peterson, A., "Vacuum-tubes and Crystal Rectifiers as Galvanometers and Voltmeters at Ultra-high Frequencies," General Radio Experimenter, Vol. 29, No. 12, May, 1945.
- Ramo, S., and J. R. Whinnery, "Fields and Waves in Modern Radio," John Wiley & Sons, New York, 1944.
- Sarbacher, R. I., and W. A. Edson, "Hyper and Ultrahigh Frequency Engineering," John Wiley & Sons, New York, 1943.
- Schelkunoff, S. A., "Theory of Antennas of Arbitrary Size and Shape," Proceedings of the Institute of Radio Engineers, 29, 493, September, 1941.
- Slater, J. A., "Microwave Transmission," McGraw-Hill Book Company, New York, 1944.

- Southworth, G. C., and A. P. King, "Metal Horns as Directive Receivers of Ultra-Short Waves," Proceedings of the Institute of Radio Engineers, 27, 95, February, 1939.
- Stratton, J. A., "Electromagnetic Theory," McGraw-Hill Book Company, New York.
- Terman, F. E., "Radio Engineers' Handbook," McGraw-Hill Book Company, New York, 1945.
- Ware, L. A., and H. R. Reed, "Communication Circuits," John Wiley & Sons, New York, 1944.
- Weber, E., "Principles of Short Wave Radiation," Electronic Industries, February, 1943.

APPENDIX

Input Impedance of Biconical Horn Antennas as Calculated
from Equation 8

	without $\frac{\lambda}{f}$ sleeve	with $\frac{\lambda}{f}$ sleeve $d = 1$ cm.	with $\frac{\lambda}{f}$ sleeve $d = \frac{\lambda}{f}$
Dipole Antenna	$z = 26.8 - j14.2$	$z = 37.0 - j19.4$	$z = 13.3 - j8.3$
$\theta = 10^\circ$ $s = 2.5$ cm.	$z = 16.0 - j26.5$	$z = 17.0 - j26.1$	
$\theta = 20^\circ$ $s = 2.7$ cm.	$z = 11.6 - j23.4$	$z = 14.6 - j26.9$	
$\theta = 30^\circ$ $s = 2.9$ cm.	$z = 12.35 - j17.5$	$z = 12.6 - j27.4$	
$\theta = 40^\circ$ $s = 3.4$ cm.	$z = 13.85 - j27.2$	$z = 12.6 - j27.4$	
$\theta = 50^\circ$ $s = 4.2$ cm.	$z = 16.5 - j8.06$	$z = 16.5 - j8.06$	
$\theta = 60^\circ$ $s = 5.2$ cm.	$z = 16.3 - j7.3$	$z = 16.35 - j8.1$	
$\theta = 70^\circ$ $s = 7.4$ cm.	$z = 56 - j8.15$	$z = 53.5 - j13.2$	
	$s = \frac{\lambda}{f}$		
$\theta = 10^\circ$	$z = 16.8 - j26.4$	$z = 9.2 - j27.7$	
$\theta = 20^\circ$	$z = 16.4 - j26.4$	$z = 27.3 - j33.6$	
$\theta = 30^\circ$	$z = 18.3 - j25.6$	$z = 24.6 - j35.4$	
$\theta = 40^\circ$	$z = 22.8 - j30.0$	$z = 30.2 - j26.5$	
$\theta = 50^\circ$	$z = 26.6 - j14.35$	$z = 30.9 - j21.0$	
$\theta = 60^\circ$	$z = 35.9 \pm j0$	$z = 37.1 \pm j0$	

APPENDIX (Continued)

	without $\frac{\lambda}{d}$ sleeve	with $\frac{\lambda}{d}$ sleeve $d = 1 \text{ cm.}$	with $\frac{\lambda}{d}$ sleeve $d = \frac{\lambda}{4}$
$\theta = 70^\circ$	$z = 88.5 + j40.5$	$z = 63 + j58$	
$\theta = 80^\circ$	$z = 1.5 + j175$	$z = 62.2 + j152.5$	
$\theta = 50^\circ, 20^\circ$	$z = 31.6 - j20.4$	$z = 15.4 - j16.9$	
$\theta = 70^\circ, 10^\circ$			$z = 5.89 + j7.2$